To the Graduate Council:

I am submitting herewith a thesis written by Vickie P. Gilbert entitled "Surface Acoustic Wave Device Designed to Monitor Frequency Shifts Due to Adsorption of Mass onto a Piezoelectric Crystal." I have examined the final copy of this thesis for form and content and recommend that it be accepted in partial fulfillment of the requirements for the degree of Master of Science, with a major in Chemical Engineering.

H D Cochran

Henry D. Cochran, Major Professor

Paul R. Bienkowski

Paul R. Bienkowski, Major Professor

We have read this thesis
and recommend its acceptance:

Joseph J. Perona

Accepted for the Council:

Lou Minkel

Associate Vice Chancellor
and Dean of The Graduate School

SURFACE ACOUSTIC WAVE DEVICE DESIGNED TO MONITOR FREQUENCY SHIFTS DUE TO ADSORPTION OF MASS ONTO A PIEZOELECTRIC CRYSTAL

A Thesis

Presented for the

Master of Science

Degree

The University of Tennessee

Vickie P. Gilbert

May 1992

ABSTRACT

Surface acoustic wave (SAW) devices have recently been utilized as extremely sensitive chemical sensors. This study was conducted to investigate the feasibility of an experimental apparatus designed to monitor, both statically and dynamically, the frequency shift in a SAW device while adsorption occurred. The apparatus was designed so that any frequency shift detected would be due solely to adsorption, not temperature or pressure differences. A Cahn microbalance was installed with the SAW apparatus to allow quantitization of the mass adsorbed onto the surface of the SAW. It was anticipated that changes in surface concentrations of less than one percent of a monolayer could be detected with this apparatus. Adsorption studies leading to frequency shift versus pressure curves were to be conducted from a total pressure of 1.0×10^{-7} torr up to atmospheric conditions and from ambient temperatures up to 45°C.

The following chapters discuss problems associated with acquiring this information and make recommendations for modifying the apparatus so that the original experimental objective may be attained.

TABLE OF CONTENTS

LIST OF FIGURES

NOMENCLATURE

C	Celsius
GP	Granville Phillips
Hz	Hertz
h	film thickness
IDT	interdigital transducers
k	constants specific to a specific type of piezoelectric material
mbar	milli bar
min	minute
RF	radio frequency
rpm	revolutions per minute
SAW	surface acoustic wave
sec	seconds
SS	stainless steel
UHV	ultra high vacuum
V	velocity
W	watts

Greek Letters

Δ	difference
λ	film Lame' constant
μ	film Lame' constant
υ	velocity

Subscripts

R	Rayleigh
$_o$	resonant

CHAPTER 1.0

INTRODUCTION AND OBJECTIVES

1.1 Introduction

In any type of separation, the interactions occurring at an interface or surface are very important. These surface phenomena occur with mass transfer across a phase, such as with adsorption, desorption, crystallization, and diffusion. Adsorption is a widely used process; it is important in gas phase applications such as separating rare gases at low temperatures, removing impurities from air feeds to low temperature fractionation, removing odors and separating low molecular weight hydrocarbons (Perry 1973). In this study, the process of physical adsorption was used with an experimental technique that utilizes a surface acoustic wave (SAW) device that may be suitable for measuring static and dynamic adsorption on solids at elevated pressures and temperatures.

This technique will be invaluable in studying processes occurring at surfaces. Exploring these processes by measuring rates of adsorption or quantifying adsorbates on the surface is often extremely difficult because many techniques currently used must be carried out under vacuum conditions and suffer from low resolution (Carberry 1987).

Infrared spectroscopy and surface-enhanced Raman spectroscopy may be carried out at elevated pressure to measure equilibrium adsorption, but their time resolution is currently inadequate for dynamic studies.

The experimental technique proposed here uses a SAW device and appears to be suitable for use at elevated pressures. This technique, which may be applicable to many processes, could help provide instrumentation for studying the fluid-solid interface that dominates many separation processes and could provide a method to study the adsorption from supercritical fluids.

1.2 Objectives

The primary objective of this study was to establish a technique for measuring adsorption equilibrium and subsequently adsorption dynamics that would be applicable at high pressures.

Several secondary objectives had to be achieved before the primary objective could be met. These objectives were:

1. To construct an apparatus that would, in an ultra high vacuum (UHV) system containing two SAW devices, selectively monitor and yield frequency shifts that result solely from mass adsorbed onto the surfaces of the SAWs. The frequency shift of the SAW transducer

offered the promise of a technique that would measure static and dynamic adsorption at high pressure.

2. To demonstrate that the apparatus functions properly by monitoring frequency shifts due to carbon tetrachloride adsorption from pure fluids and in argon/carbon tetrachloride binaries as a function of temperature, pressure, and composition.

3. To construct an apparatus that would allow one to quantify the mass of gas adsorbed onto the quartz plate (SAW device) and to calibrate that mass amount to a frequency shift.

4. To establish that the frequency shift due to mass adsorbed was measurable and that any frequency shift due to temperature change or gas density change were negligible or could be calibrated and corrected for in final equations describing the process.

CHAPTER 2.0

BACKGROUND

Piezoelectric quartz crystals have long been used as frequency and time standards and as selective filters in electronics. Other less obvious uses are for determining the dew point of gases (Dyke 1945) and for measuring temperature (Flynn, et al. 1962). An early study by Sauerbrey, using piezoelectric quartz crystals, showed the relationship between the weight of a metal film deposited on a crystal and its effect upon the resonant frequency of the piezoelectric crystal (Sauerbrey 1959). Ho and Guilbault used quartz crystals to detect hydrocarbons in the atmosphere (Ho and Guilbault 1980). In Ho's study and in the following ones mentioned, a selective coating was placed on the surface of the piezoelectric substrate in order to absorb and thereby detect and measure specific compounds (a selective coating is not applied in the present study). Other studies using piezoelectric substrates, specifically SAW devices, include the use of the device to detect organophosphorus compounds (Guilbault, Affolter, and Tomitao 1981), to sense hydrogen (D'Amico, Palma, and Verona 1983),

and as a gas chromatography detector (Wohltjen and Dessy 1979).

Many of the earlier uses of piezoelectric crystals utilized bulk wave devices such as sorption detectors (King 1964; Slutsky and Wade 1962). Slutsky and Wade's work demonstrated that a polished piezoelectric crystal could be used as a specialized, highly sensitive method for determining adsorption isotherms of argon and hexane. This study also discussed related thermodynamic quantities, such as dielectric constants and thermal effects, which influence the operation and results of the device (Slutsky and Wade 1962).

The bulk wave device has proven to be a valuable tool in the scientific field and will continue to be used. However, there are several differences between a bulk wave device and a SAW device that, for the present study, make the SAW device a much more valuable research tool. The bulk wave device operates at orders of magnitude lower frequencies than does the SAW device; the sensitivity of the bulk wave device depends on the diameter and thickness of the piezoelectric substrate, while energy transport in the bulk wave device occurs throughout the substrate. Bulk waves have their energy directed along the boundary of the substrate but their propagation vector is tilted into the substrate (Auld 1973).

Later applications of piezoelectric crystals as detectors have, in some cases, used SAW devices. The SAW oscillator, first reported by J. D. Maines, et al. in 1969, was originally used to measure the temperature coefficient of SAW delay times in lithium niobate (Maines, et al. 1969). Since that time the SAW device has been used in many different applications, specifically in the detection of various chemical compounds (e.g., as a tool for sensing hydrogen and as a gas chromatography tool, as previously mentioned).

In a SAW device, Rayleigh waves propagate along the surface of a semi-infinite substrate. These waves have fields that fall off exponentially in amplitude away from the surface and that need both shear and longitudinal wave components to satisfy the boundary conditions in the mathematical problem setup (Kino 1989). Rayleigh waves have most of their energy localized within one or two acoustic wavelengths of the surface (Wohltjen 1984).

The SAW device is more sensitive than the bulk wave device because its sensitivity is directly related to its resonant frequency. A SAW device operating at 300 Mhz can easily be fabricated (Lewis 1974), while a bulk wave device operating at this frequency would be impossible to fabricate. Because the frequency shift is directly proportional to the square of the resonant frequency

($\Delta f \propto f_o^2$) for both cases (Wohltjen 1984), it is obvious why the SAW device is more sensitive.

A comparison done by Bryant et al., has shown that the SAW, used to detect SO_2 is at least an order of magnitude more sensitive than the bulk wave sensor used in the detection of SO_2 (Bryant, Lee, and Vetelino 1981). In one comparison done by Wohltjen, a SAW device composed of ST quartz was found to produce a frequency shift of more than 200 times greater than the 15 Mhz bulk wave device employed by Sauerbrey (Wohltjen 1984; Sauerbrey 1959).

The advantages of the SAW device over other types of oscillators are summarized below:

1) The delay line, an interdigital transducer at each end of an appropriate piezoelectric substrate, is a small, inexpensive planar component that may be rigidly mounted, making it very rugged (Lewis 1974).

2) The sensitivity and size of the SAW delay oscillator is directly related to its resonant frequency.

3) The SAW device is capable of operating at frequencies that are at least two orders of magnitude higher than the bulk wave device and is therefore much more sensitive.

4) The frequency of oscillation is determined by the transducer pattern and not by any dimension of the quartz crystal. The crystal can therefore be made thick and mounted securely to give good mechanical and thermal contact to the header, which improves stability (Lewis 1974).

5) By use of reference SAWs, temperature drift compensation may be achieved, allowing one to choose the crystal substrate based more upon the coupling efficiency of the applied radio frequency voltage to the mechanical deformation than on the temperature coefficient of delay of the substrate.

6) The devices are easily fabricated by application of thin metallic coating and subsequent etching with a photolithographic technique.

7) The small size, electronic output, and adaptability of the device make it attractive for applications in many areas (Wohltjen 1984).

8) Compared to its bulk acoustic wave analog, a SAW device has the advantage, (because its energy is concentrated at the substrate surface) of being

accessed, focused, reflected, and influenced easily, which leads to wide design flexibility (Konstantinov and Hess 1980).

Disadvantages associated with the SAW include:

1) Temperature sensitivities of certain orientations of piezoelectric substrates may require "corrections" in order to calculate the actual frequency shift occurring due to mass adsorption (Mason 1954).

2) The possible shift in orientation of the substrate as mass is added to its surface could possibly alter the temperature coefficient of delay. This is a problem only with certain orientations of some crystals. However, if a shift occurs, it could lead to false results unless the change in the temperature coefficient is noted in final calculations or corrected for in the apparatus design. This is a problem only when coatings are applied to the piezoelectric material (i.e., metal coatings in the form of electrodes or organic coatings for selective adsorption which exceed the limitations of having no effect upon resonant frequency, etc.) prior to adsorption.

CHAPTER 3.0

THEORY

A simple SAW transducer may be composed of a piezoelectric crystal onto which an interdigital transducer (IDT), which converts an electrical signal into a surface acoustic wave and reconverts it to an electrical signal, has been applied (Figure 3.1). Typically, the IDTs are deposited onto the surface of the substrate by photolithographic techniques consisting of evaporation, under vacuum conditions, of a metal surface like gold, through a photoresist mask. This mask has usually been prepared photographically and its size reduced several fold so that it meets the desired size requirements for the device being fabricated (Kino 1989).

When an electric potential is applied to the electrodes (IDTs) on the surface of a piezoelectric crystal, an electric field is produced. A net stress is created in the piezoelectric material when the electric field is applied due to unequal movements of dipoles (moving different distances) in the direction of the application of the electric field (Figure 3.2 illustrates this process.) Thus, the crystal develops net stresses. These stresses cause a

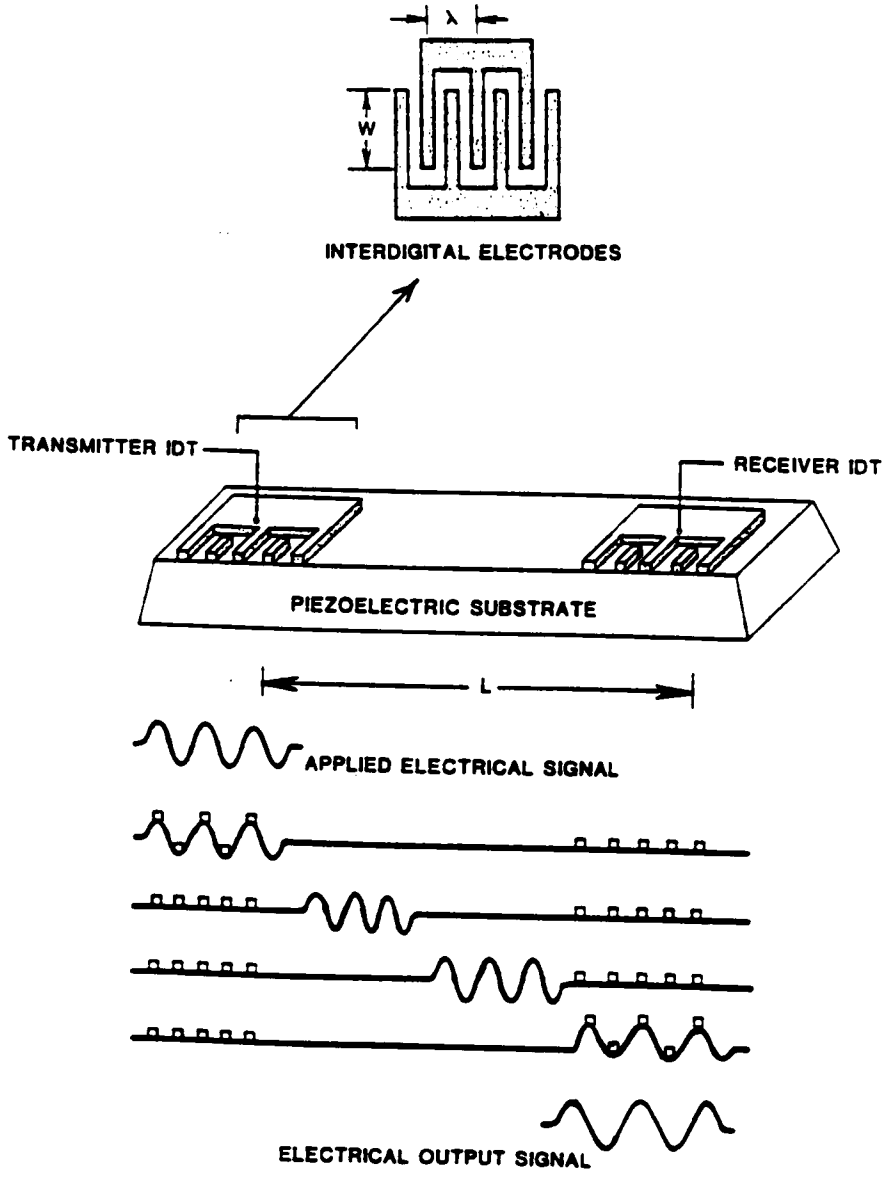

Figure 3.1 Interdigital Electrodes and Propagation of SAW

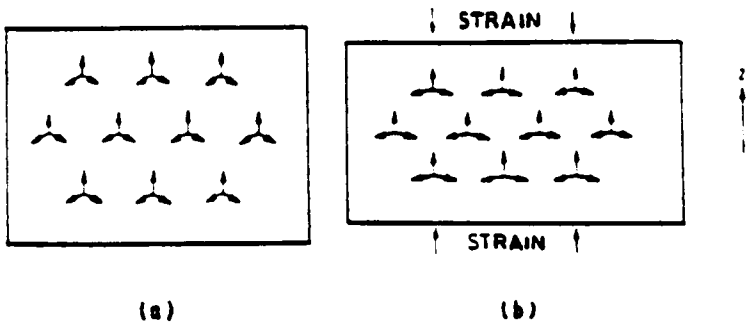

(a) The unstressed crystal has a threefold symmetry axis. The three arrows represent a group of ions with a triple charge, a positive charge at each vertex and single negative charges at the arrowheads. The sum of the three dipole moments is zero. (b) When the sample is stressed so that the dipole moment is finite, there is no longer threefold symmetry (Kino 1989).

Figure 3.2 Schematic of Dipoles in a Piezoelectric Crystal

mechanical deformation, by which means a surface acoustic wave is generated (Figure 3.1).

A second IDT or system of IDTs acts as receiver(s) of energy from the excited surface acoustic wave thus generated. A single pair of electrodes cannot excite surface acoustic waves very efficiently, so IDTs typically consist of several pairs of electrodes or fingers placed in a specific pattern. The finger width and spacing of the IDTs determines the frequency and bandwidth of the surface acoustic wave that the electric field generates. With proper spacing between the fingers, the initial wave reaches the second pair of electrodes just as the signal is repeating in that pair. The pattern is designed so that each wave created by a single pair of electrodes reinforces other waves. By proper choice of the spacing between fingers (each finger pair should be one wavelength), a large acoustic signal is created (Kino 1989). The electrode fingers and the space between the two sets of electrode fingers are called the delay line and is the surface area where adsorbed mass affects the resonant frequency of the SAW device. Figure 3.1 shows 'L' as the length of the delay line on this particular piezoelectric substrate. Based on the pattern of IDTs applied to the surface, each crystal has a specific resonant frequency generated.

Basically, two types of waves are important in acoustic wave propagation: longitudinal waves in which the motion of

particles in the substrate is in only the direction of propagation of the wave, and shear waves where the movements of particles in substrate or acoustic medium is transverse to the direction of propagation (Figure 3.3). Several different modes of wave propagation are possible in the acoustic wave guide, such as: (1) shear horizontal waves (particle motion in one direction), (2) Love waves, which are shear waves that are polarized parallel to the substrate boundaries, (3) Lamb waves, which are the coupled wave vectors of the shear and longitude particle waves and have the same propagating component along a single axis, and (4) Rayleigh waves, or surface acoustic waves, which propagate along the surface and consist of a mixture of shear and longitudinal stress components. Rayleigh waves are analogous to waves on the surface of water since wave motion is strong at the surface and falls off internally just as Rayleigh waves fall off exponentially away from the surface. There is no restoring force at the surface of a solid medium, the piezoelectric crystal, and any force normal to the surface must be zero; therefore the components of stress must be zero at the surface. In a wave propagating in the direction of infinite length (the z direction) in a semi-infinite medium, the total energy per unit length in the wave must be finite and the field components of the wave will fall off exponentially into the interior of the substrate (Kino 1989). Figures 3.4 through 3.7 illustrate the propagation of the types of waves mentioned above.

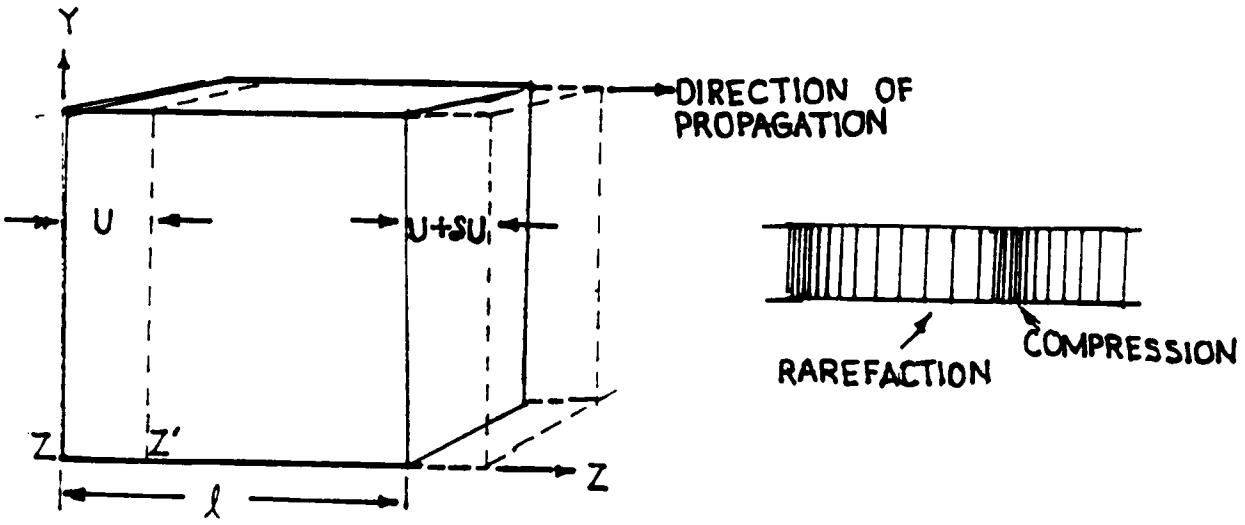

Longitudianl Wave

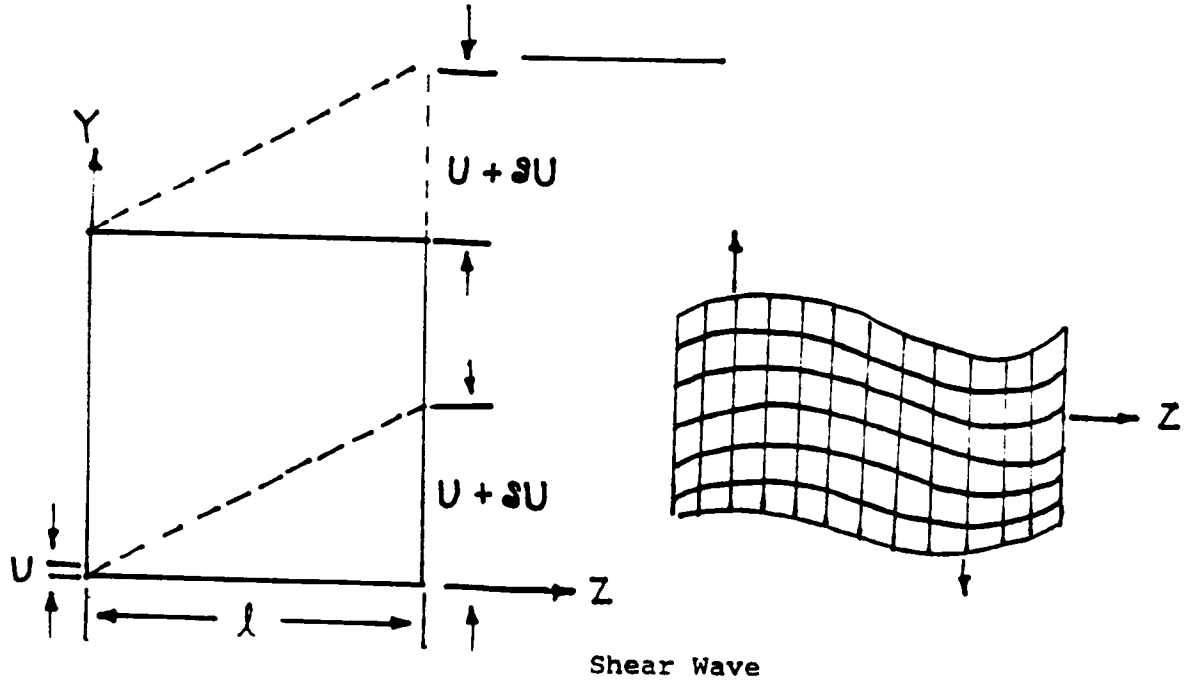

Shear Wave

Figure 3.3 Longitudinal and Shear Wave Propagation

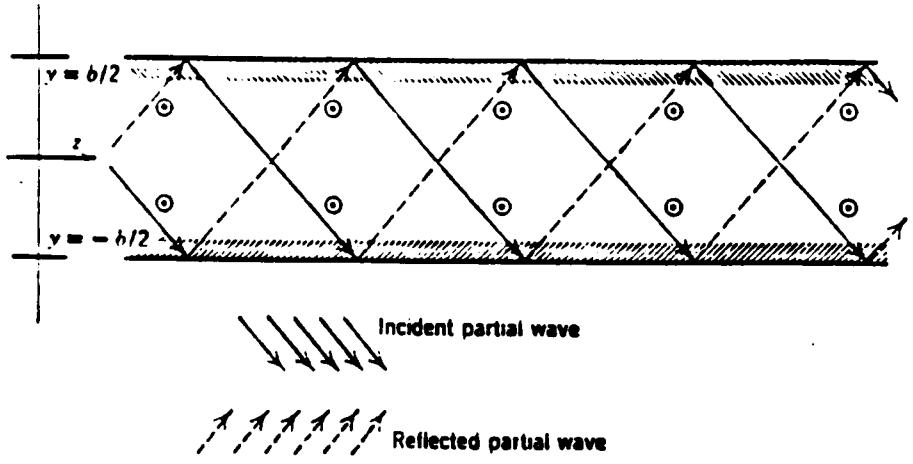

Figure 3.4 Partial Wave Pattern For Transverse Resonance Analysis of Shear Horizontal Wave Propagation on an Isotropic Plate (Kino 1989)

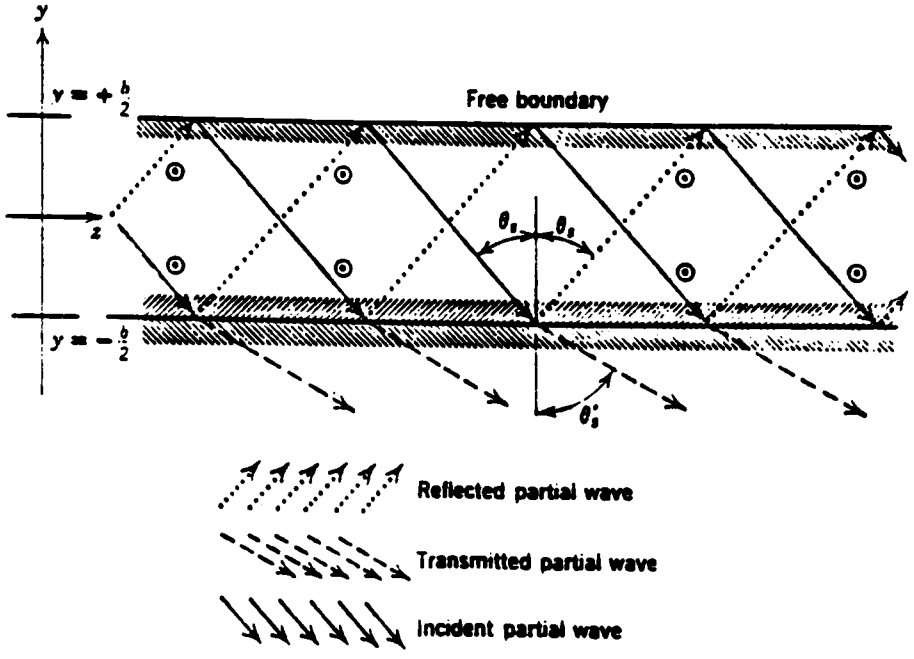

Figure 3.5 Partial Wave Pattern For Transverse Resonance Analysis of Love Wave Propagation on an Isotropic Plate (Kino 1989)

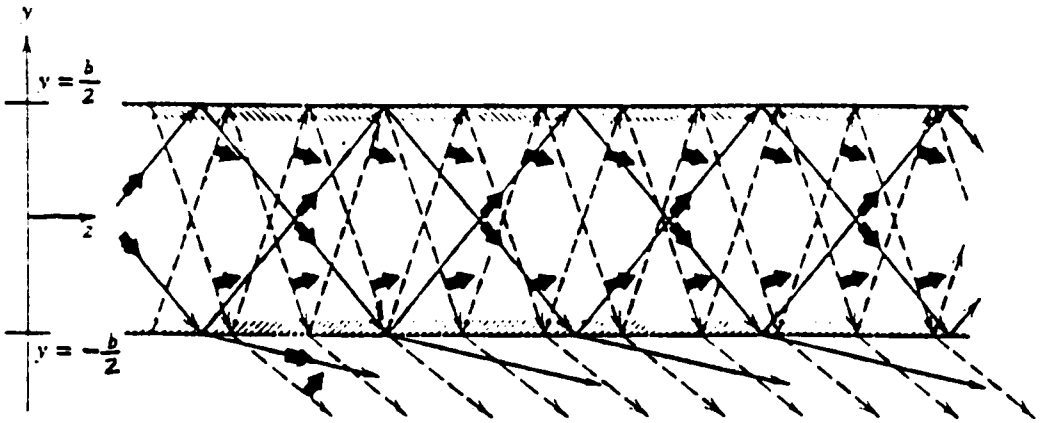

Figure 3.6 Partial Wave Pattern For Generalized Lamb Waves on an Isotropic Plate (Kino 1989)

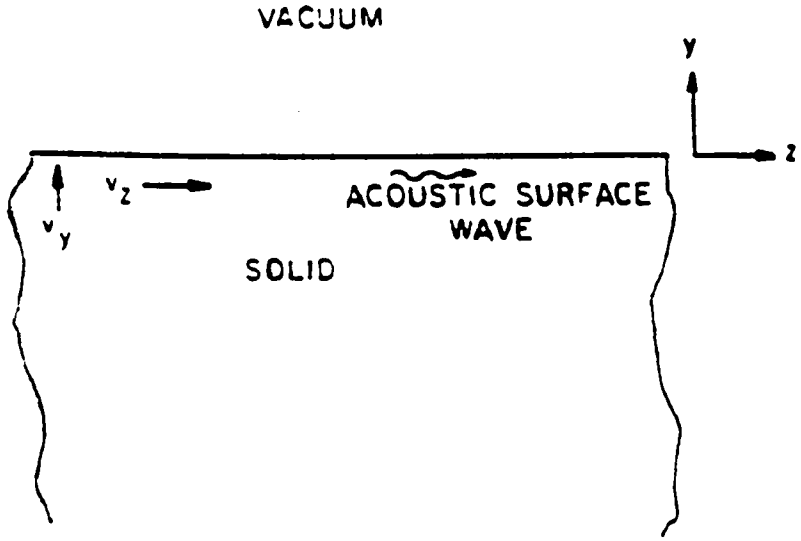

Figure 3.7 Rayleigh Wave Pattern (Kino 1989)

By controlling the geometry of the IDT during its deposition upon the surface of a piezoelectric substrate, one can prepare a transducer with which the Rayleigh wave can be easily excited and detected. In Rayleigh waves, the longitudinal and shear fields are bound to the surface of the substrate so that the interior of the substrate is left unperturbed. Penetration of the Rayleigh wave into the substrate is only one to two wavelengths (Auld 1973). This wave and its characteristics allow for the greatly increased sensitivity of the SAW device over the bulk wave devices, which operate by totally different wave mechanisms.

SAW devices may be fabricated upon many different types of piezoelectric substrates. Typically quartz or lithium niobate crystals are used because of their availability, low cost, good piezoelectric coupling, and for specific types, low temperature coefficients of delay (Bryant et al. 1983; Wohltjen 1984). The frequency of a SAW oscillator varies with temperature as follows:

$$f \approx f_0[\ 1 - 3 \times 10^{-8}\ (T - T_0)^2]$$

where f_0 is the maximum frequency occurring at temperature T_0.

ST quartz exhibits a frequency change of zero ppm at temperatures near ambient (Lewis 1974).

Different crystalline orientations will exhibit one or more, but not all, of these advantages. ST quartz, which was used to fabricate the SAW devices employed in the

present examination, has a zero temperature coefficient at room temperature. The orientation of ST quartz is 42° 45′ off the Y axis (Figure 3.8). As mass in the form of IDTs is deposited upon the crystal's surface, the original orientation of the quartz may have to be altered to compensate for the additional mass so that the temperature coefficient may remain zero under ambient conditions. Typically this is done by the SAW manufacturer. Depending on the amount of material added to the surface of the quartz the orientation of the quartz may vary from 32° to 42° 45′.

The major cause of any acoustic wave attenuation in solids and liquids is due to the viscous dissipation between adjacent particles of the substrate and adjoining media. Attenuation is proportional to the square of the resonant frequency (attenuation $\propto f_o^2$) and inversely proportional to the wave velocity (attenuation $\propto 1/V_R$) (Wohltjen 1984).

Other interactions may also occur to cause the wave energy to be redirected away from the receiving IDT. These interactions may be due to scattering, caused by crystal imperfections, and phonon-electron interactions. Energy losses of these types are usually small and constant with time and moderate temperature variations (Wohltjen 1984). The effects of reflected energy may be alleviated by the application of an acoustic energy absorber at the ends of the delay line or by cutting the ends of the piezoelectric crystal at an angle so that phase coherence of the

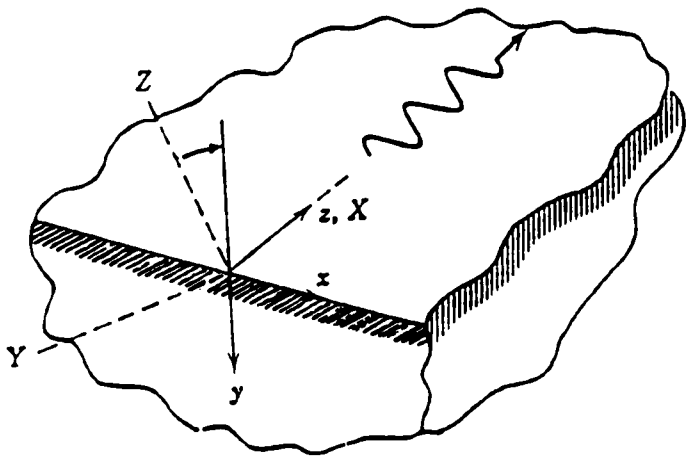

Figure 3.8 Schematic Illustrating the Orientation of ST Quartz. X, Y and Z are crystal axes; x, y and z are coordinate axes.

wave is destroyed. Scattering, due to imperfections, may cause a SAW to become a bulk acoustic wave that can reflect from the bottom of the substrate and interfere with the Rayleigh waves propagating across the surface. Again, an absorbing material may be added or grooves cut into the base of the substrate to prevent this problem. In addition to the these losses, thermal conduction, which also varies as the square of the frequency, may cause energy loss for acoustic waves (Wohltjen 1984).

Because the energy of a Rayleigh wave is concentrated within one to two wavelengths from the surface, a device operating with SAWs is an ideal mechanism to measure adsorption for the following reasons:

(1) Adsorption occurs on the surface of the polished isotropic piezoelectric material and adds mass to the surface.

(2) Any viscous dissipation acting near the surface of the crystal would cause some attenuation of the resonant frequency of the device(i.e., the additon of mass causes the amplitude, phase, velocity and frequency of the piezoelectric material to attenuate causing a frequency shift).

(3) Depending on the resonant frequency of the device, a frequency shift of 1 in 10^8 Hz or better may be measured if the baseline noise is maintained at 1 part in 10^7 (This is typically easy to do).

Wohltjen and Dessy have shown that monitoring the changes in SAW velocity (by measuring frequency perturbation) can be much more precise than measuring the amplitude or phase changes because of the accuracy of frequency measurements that can be made (Wohltjen and Dessy 1979).

The relationship between the resonant frequency of a SAW device and the change in that frequency due to mass adsorbed onto its surface may be examined by means of perturbation theory. Perturbation theory is concerned with small changes in a solution of a problem due to small changes in the parameters comprising the problem. For waves, the perturbation theory states that the total field in a perturbed medium is very similar to the field of a wave in an unperturbed medium.

Auld has presented several examples of the velocity changes and hence Δf due to surface loading of a SAW device by : (1) a thin lossless isotropic overlay, (2) a thin lossless anisotropic overlay and (3) Rayleigh surface wave attenuation due to surface loading by a nonviscous bulk gas or liquid. Development of the final equations presented is

for the first case mentioned. Others may be found in Auld's description of the perturbation analysis of a SAW device (Auld 1973). His analysis yields the following equations:

$$(1)\quad \frac{-\Delta V_R}{V_R} = \frac{V_R h}{4P_R}\left[\rho'|v_{Ry}|^2 + \left[\rho' - \left[\frac{4\mu'}{V_R^2}\right]\left[\frac{\lambda' + \mu'}{\lambda' + 2\mu}\right]\right]|v_{RZ}|^2\right]_{Y=0}$$

where $\frac{(v_{RY})_{Y=0}}{\sqrt{P_R}}$, $\frac{(v_{RZ})_{Y=0}}{\sqrt{P_R}}$ are the normalized particle velocity components at the surface

ρ' - mass density

μ' and λ' - Lame' constants

h - film thickness

V_{Ry}, V_{Rz} - Rayleigh wave velocity in the y and z directions

P_R - particle in motion in the Rayleigh wave

R_Z and R_Y - Rayleigh waves in the z and y directions

These parameters may be evaluated analytically in terms of the properties of the substrate.

For the current study, the aspect of a nonuniform adsorbed surface does not influence the result because the material adsorbed onto the surface of the SAW device would be extremely thin and uniform. The thickness would be less than one percent of a wavelength, which is approximately 28 μm for the 112 Mhz SAW device. The nude surface of the SAW device is also considered isotropic.)

Wohltjen has shown that Auld's equation may be simplified by making the following substitutions:

$$C_1 = (-V_R\ |V_{RY}|^2_{Y=0})/4P_R, \text{ and } C_2 = (-V_R\ |v_{RZ}|^2_{Y=0})/4P_R$$

Then,

$$(2)\quad \Delta V_R/V_R = (C_1 + C_2)h\rho' - C_2h\left[\left[\frac{4\mu'_r}{V_R^2}\right]\left[\frac{\lambda' + \mu'}{\lambda' + 2\mu}\right]\right]$$

The normalized particle velocity components are dependent on the resonant frequency of the SAW device and thus act as a constant, k, which must be multiplied by the wave frequency, $C_1 = k_1 f_0$ and $C_2 = k_2 f_0$. Hence, the equation will be simplified to:

$$(3)\quad \frac{\Delta V_R}{V_R} = (k_1 + k_2)f_0h\rho' - k_2fh - \left[\left[\frac{4\mu'}{V_R^2}\right]\left[\frac{\lambda' + \mu'}{\lambda' + 2\mu}\right]\right]$$

at quiescent resonant frequency $\Delta V_R/V_R = \Delta f/f$, where

Δf - change in the resonant frequency due to a small perturbation
by a thin film overlay.

If the perturbation is small, then $f - \Delta f \simeq f$ and

$$(4)\quad \Delta f = (k_1 + k_2)f^2h\rho' - k_2f^2h\left[\left[\frac{4\mu'}{V_R^2}\right]\left[\frac{\lambda' + \mu'}{\lambda' + 2\mu'}\right]\right]$$

Rayleigh waves act most like shear waves. The shear modulus-dependent portion of the above equation becomes negligible when $4\mu'/V_R^2$ is less than 100 as it is for soft polymers, for example. Therefore the equation reduces to a simplified relationship,

(4) $$\Delta f = (k_1 + k_2) f^2 h\rho'$$

where, $h\rho'$ - the mass/area of film adsorbed (Wholtjen 1984).

Here we note that $\Delta f \propto f^2$ just as has been shown by King (King 1964) from Sauerbrey's original development of the equation concerning bulk wave acoustic devices. Frequency change is highly dependent on the resonant frequency of the SAW device and increases with the square of the resonant frequency. Frequency change is also proportional to the mass adsorbed per unit area.

Temperature will have some effect upon the constants comprising Auld's original equation but if the last portion of equation (1), the stress components, remains less than 100, the only effect of temperature will be on the density of the material adsorbed and any change in frequency response of the crystal itself due to a non-zero temperature coefficient.

CHAPTER 4.0

EXPERIMENTAL

4.1 EQUIPMENT AND OPERATIONS

4.1.1 Apparatus and Approach

To assess the potential of the surface acoustic wave (SAW) device for measuring adsorption and desorption rates, equipment was assembled for determining the change of frequency in the surface waves propagating across a SAW device and for separating out the effects caused by surface loading on the crystal from other factors that might influence the frequency (e.g., temperature and pressure changes). A system was set up to ensure that constant temperature and pressure could be maintained within the system. A reference SAW was used with an experimental SAW to alleviate many of the problems associated with temperature and pressure changes (Figure 4.1 is a schematic of the apparatus). Ideally, the symmetric sides of the system are maintained at exactly the same temperature and total pressure. Only the partial pressure of the adsorbing gas would be different on the experimental side of the apparatus. The apparatus permits Δf to be measured by mixing the frequency signals from the reference and the

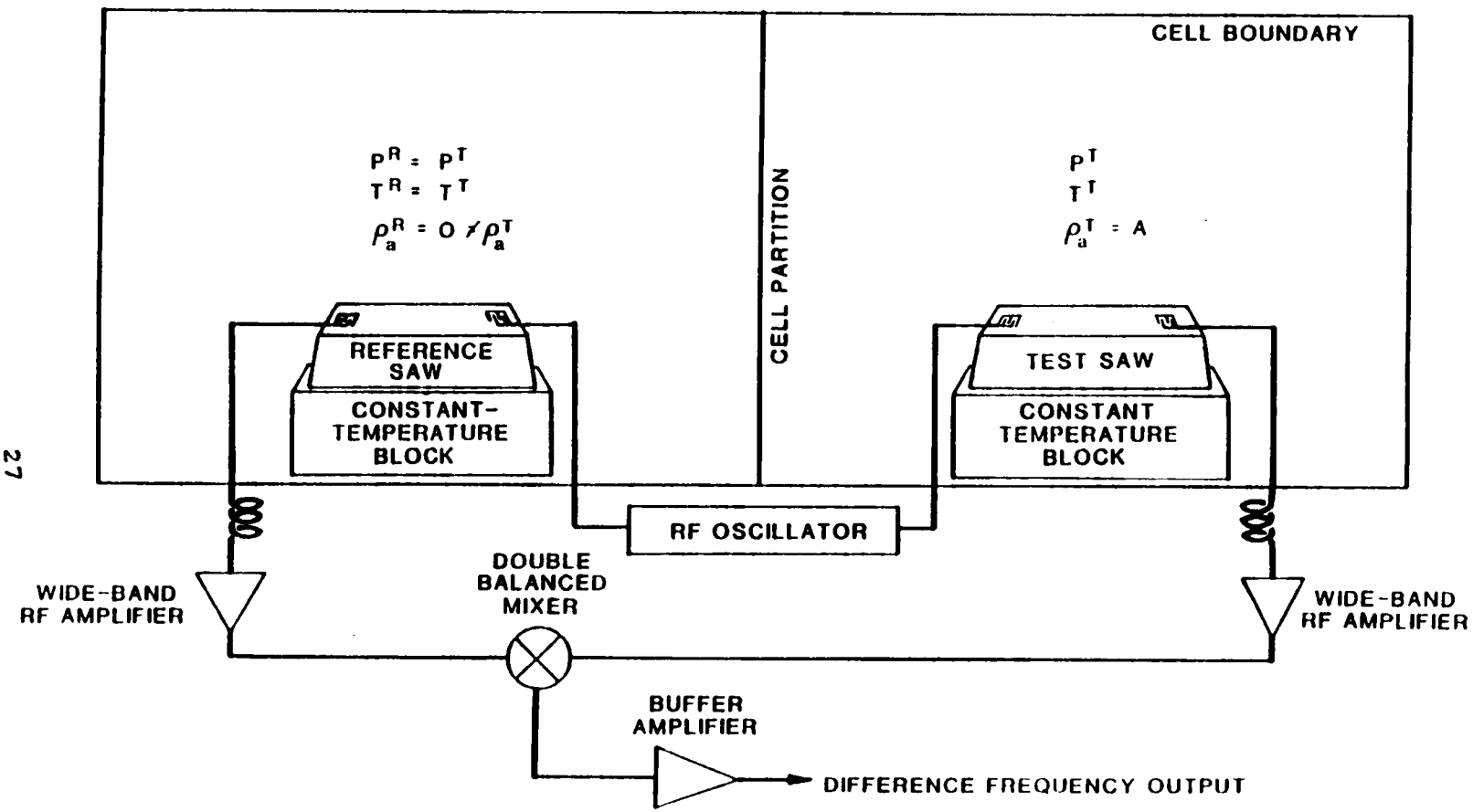

Figure 4.1 Schematic Showing Diagram of Experimental SAW Apparatus

experimental SAW devices so that Δf results from the interference of the two frequencies. Since Δf is expressed as a "difference" frequency, this difference could only be due to mass adsorbed because all other parameters are identical. The goal of these design features was to obtain frequency differences due solely to adsorption. The experimental approach was to use a dual delay line as typical of the chemical sensor described in the literature (Wohltjen 1984; D'Amico, Palma, and Verona 1982; Chuang, White and Bernstein 1982) but with modifications that would allow for application of the apparatus as a means of measuring equilibrium adsorption and dynamic adsorption rates. The major difference was that the two delay lines would not be adjacent to one another (located on the same substrate crystal) yet would be under identical conditions of temperature and total pressure and that neither delay line would be coated with a selective coating for preferential adsorption.

The apparatus developed from the above approach consisted of several units: (1) the vacuum system, (2) the pressure/flow control system, (3) the temperature control system, (4) the SAWs, and (5) the Cahn microbalance unit. The ultra high vacuum (UHV) system permitted study of the adsorption of a gas of controlled composition and pressure onto a surface of reproducible cleanliness. It housed the SAW devices, delineated the pathway of gas flow to be used

for adsorption studies, and was the basic structural unit for the entire experimental apparatus. The symmetrically designed vacuum system consisted of a reference and an experimental side, both pumped by a central turbomolecular pump. The pressure and flow control system was built into the UHV system and, by a series of valves and flow controllers, maintained a constant total pressure and yet allowed the partial pressure of an adsorbing gas to be modified. The flow control mechanisms allowed separate control of the gas flow to each SAW and also aided in the evacuation of the entire vacuum system during bakeout. An air bath temperature control system surrounded the entire ultra-high vacuum (UHV) apparatus with the exception of the pumps and the electronics associated with the pressure control system. Its purpose was to ensure uniform temperature of the SAWs during ambient temperature changes. The primary components of the experimental apparatus were two SAW devices, designed to measure the frequency shift due to adsorption (Figures 3.1 and 4.2). Two identical SAW devices were used: the reference SAW in the portion of the system exposed to a nonadsorbing gas, and the experimental SAW in the portion of the system exposed to the adsorbing gas. The frequencies of the two delay lines were mixed to yield a difference frequency that would be due solely to the mass loading on the experimental SAW. The fifth component of the experimental apparatus was the Cahn microbalance,

112 MHz DUAL SAW DELAY LINE

(PART NO. SD-112-B)

Taken from Microsensor, Inc. Catalogue

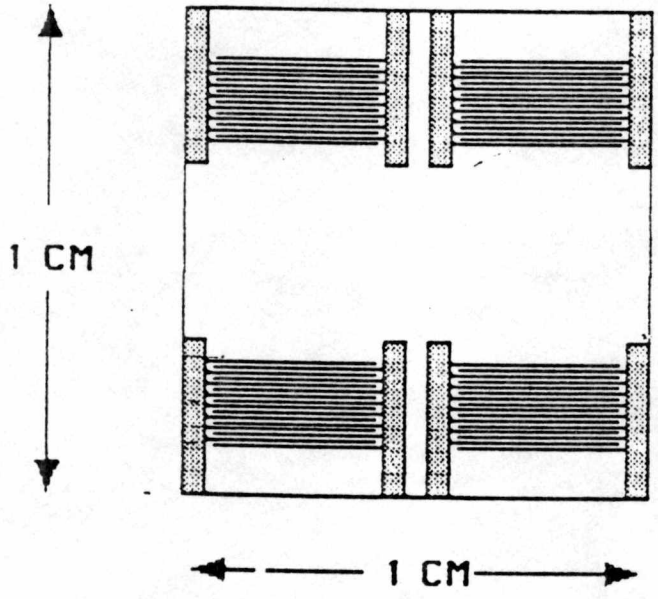

ELECTRODE MATERIAL	:	GOLD
SUBSTRATE MATERIAL	:	ST-QUARTZ
FINGER WIDTH	:	7 MICRONS
FINGER SPACING	:	7 MICRONS
NO. OF FINGER PAIRS	:	50
ACOUSTIC APERTURE	:	2240 MICRONS

Figure 4.2 112 MHz Surface Acoustic Wave Device

which allowed one to quantitate mass adsorbed onto the surface of the ST quartz samples to 0.1 μg under the same conditions as the ST quartz SAW device. The Cahn microbalance was included to correlate the quantity of mass adsorbed versus frequency shift obtained with the SAWs.

The following paragraphs discuss the specfics of each portion of the apparatus as it was designed.

Vacuum System

The primary purpose of the UHV was to ensure that adsorption occurred onto a surface of reproducible cleanliness. The UHV system that houses the SAWs and contains both the pressure and flow control mechanisms and the microbalance was designed to ensure that frequency shifts, as measured by the SAW devices, would be due solely to the adsorption of the gas, of known composition and pressure, under study.

Because of the UHV conditions, any adsorbing impurities that were present would adsorb at a slow rate compared with the rate of adsorption of the test gas. At higher pressures, the surface would have been rapidly covered by any adsorbing impurity such as water.

Figure 4.3 shows the main body of the UHV system, which was built of 316 stainless steel (SS) vacuum components that were 1.5-inch i.d. with standard conflat flanges throughout most of the system.

M1, M2 - manual control valves (open, shut types)
V1, V2 - Varian variable leak valves
L1, L2, R1, R2 - Varian right angle vales for directing flow of gas
T1 - Varian tee valves
GP1, GP2 - Granville-Phillips control valves

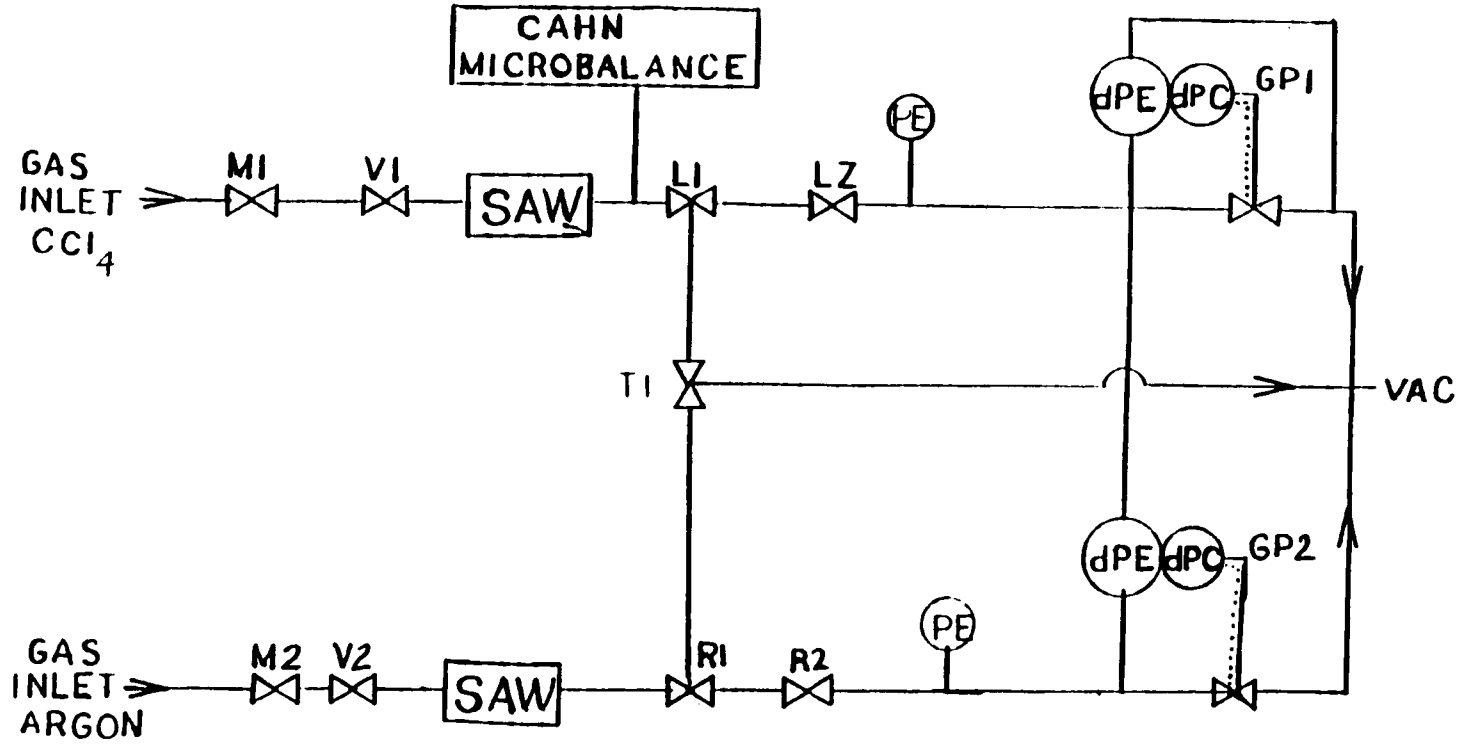

Figure 4.3 Ultra High Vacuum and Flow Control System

(Connections to the Granville-Phillips (GP) control valves were made of 0.25-inch SS tubing.) By constructing the vacuum system of stainless components connected with copper gaskets, a bakeout at 450°C was obtainable with high temperature heating tapes. This allowed a greater assurance of cleanliness of the vacuum system and the various components that it housed.

After initial bakeout, ultra high and high vacuum conditions were maintained by using a Leybold Heraeus turbomolecular vacuum pump, model TMP150, with pumping speed of 145 L/s for nitrogen and 115 L/sec for hydrogen. The ultimate pressure attainable with this pump is less than 1.0×10^{-10} mbar ($<7.5 \times 10^{-9}$ torr); its rotational speed is 50,000 rpms. The turbomolecular pump was backed by an Edward's rotary vane roughing pump, model E2M8. Alone, the roughing pump is capable of attaining a vacuum of 7.5×10^{-2} torr. A zeolite sorption trap, Leybold Heraeus model FA2-4, was located between the turbomolecular pump and the roughing pump to prevent backflow of oil vapors from the roughing pump into the vacuum system. Varian right angle and tee valves, with conductances of 32 L/sec for 1.5-inch valves, fully open, were used to control the pathway of gas flow in the UHV system and subsequently onto the SAWs.

Pressure And Flow Control

Figure 4.3 also shows the components of the pressure control system. Flow and pressure were controlled manually when the pressure ranged from 1.0 X 10^{-8} to 1.0 X 10^{-3} torr. At higher pressures, an automatic control system was utilized. Each of the components associated with the pressure/flow control system, except for the electronics and pumps, was maintained in a constant temperature air bath, which is described in the next section.

At the lowest pressures monitored in the system (i.e., 1.0 X 10^{-8} torr), a manual flow/pressure control setup was used. This system consisted of two Varian variable leak valves and two Varian nude ionization gauges and their respective controllers. Figure 4.3 illustrates the basic setup of both the automatic and manual pressure/flow control systems. Figure 4.4 lists the components of the pressure control system and their respective specifications.

In the lower pressure ranges, 10^{-6} to 10^{-5} torr, the pressure drop across the two GP valves was great enough to allow no detectable change in pressure on one side of the system when flow was increased to the opposite side for several minutes, thus allowing for flow control of the non-adsorbing and adsorbing gas separately. (Initial pressure readings for the entire system were in the 1.0 X 10^{-8} to 1.0 X 10^{-7} torr range). When R1 and L1 (Figure 4.3) were closed and flow was forced through the GP valves, the pressure rose

Leybold Turbomolecular Pump (150)	Pumping speed for H_2 - 340L/sec	Rotary speed 45,000 rpm	Ultimate vacuum $<10^{-9}$ mbar	Temp. Range 0 to 45°C
Edward's Rotary Pump	98 m^3/hr		2.5 X 10^{-4} mbar	to 67 °C
Cahn Microbalance	Precision $\pm 10^{-5}$ of total load	Accuracy $\pm$ 0.1% of recorder range	Weighing Range 10 μg - 1 g	Bakability 100 °C
Sargent-Welch Thermonitor	Sensitivity $\pm$ 0.001°C	Proportional Power output 1000 W	Auxiliary Power output 500 W	
MKS Pressure Sensing Head	Type of measurement Absolute and Differential	Accuracy 0.001% of reading	Pressure Range 10 and 1000 torr X 0.1, 0.01	Temp. Range ambient to 450°C
MKS Signal Conditioner	Vacuum Range 25 K to 1mm Hg times 1, 0.1, 0.01	Temp. Range 15 to 45 °C		
Varian Variable Leak Valve	Vacuum Range atmosphere to 10^{-11} torr	Minimum Leak Rate 1 X 10^{-9} torr L/sec	Temp. Range to 450 °C	Material 300 Series SS

Figure 4.4 Equipment Specifications for SAW Apparatus Vacuum System

Varian Right Angle Valve	Vacuum Range atmosphere to 10^{-11} torr	Conductance 32 L/sec	Temp. Range to 450 °C
Varian Ionization Gauge Control Unit	Pressure Range 1 to 10^{-11} torr	Stability ± 25% of full scale	Temp. Range 20 to 50 °C 100 °C (cables)
Varian Ionization Gauge (Milli and UHV)	Pressure Range 0.6 to 2 X 10^{-11} torr	Sensitivity .5/torr and 25/torr	Temp. Range to 450 °C
Granville-Phillips Servo Driven Valve	Pressure Range 1000 to 10^{-11} torr	Conductance to vacuum, $<10^{-12}$ L/sec	Material Monel/304 SS
Granville-Phillips APC Controller	Sensitivity < 1±%	Accuracy > ±1% at 0 to 50 °C	Temp. Range 0 to 50 °C

Figure 4.4 continued

to the 1.0 X 10^{-5} torr range. For manual control, right angle valves R1 and L1 and the tee valve were closed, preventing backflow of the adsorbing gas onto both SAW surfaces. Visual monitoring of the pressure output from the Varian ionization gauges was used as a basis for adjusting the two variable leak valves controlling the flow of the adsorbing gas and the nonadsorbing gas. The relative pressure difference between the reference and experimental side of the apparatus could be maintained at less than two percent for several minutes by manual control.

The automatic control contained with the UHV system was utilized for operating pressures greater than approximately 1.0 X 10^{-4} torr. This pressure/flow control mechanism included two GP control values, a 10 torr MKS sensor head, a 1000 torr MKS sensor head along with the electronics necessary for their operation, and the electronics necessary for the operation and maintenance of a particular pressure set point utilizing the GP control valves (Figure 4.3).

The 1000-torr pressure transducer, model 315BH, was used as an absolute pressure-sensing device. The 10-torr head, model 315BH, was utilized as a differential pressure transducer for maintaining equal pressures on both the experimental and reference sides of the vacuum system. Both pressure-sensing devices were connected to MKS high-accuracy signal conditioners through which connections were made to the two GP valves and their controllers. Basically, the

valves work by accepting an incoming DC voltage signal from the pressure transducer, comparing the incoming signal to the set point established by the experimenter, generating an appropriate error signal, and then using the error signal to activate the GP control valves.

When a mixture of adsorbing and nonadsorbing gas was utilized in the experimental side of the apparatus, the container of pure adsorbing gas, as a liquid, was sparged with nonadsorbing gas to create a saturated mixture. Temperature control determined the partial pressure of the adsorbing gas. Figure 4.5 shows a more detailed setup of the boiling flask and its attachment to the UHV system and nonadsorbing gas source. The automatic pressure/flow control mechanism was employed as described previously to maintain a desired total pressure in the system.

Temperature Control

Figure 4.6 is a schematic of the temperature control system. Stringent temperature control was necessary to alleviate false frequency shifts obtained due to small temperature differences between the two SAWs. The purpose of the temperature-controlled air bath was to ensure uniform temperatures around both SAWs and to maintain a desired constant temperature throughout the entire vacuum system.

The vacuum apparatus was housed in a Marinite box, a material that has properties similar to asbestos for

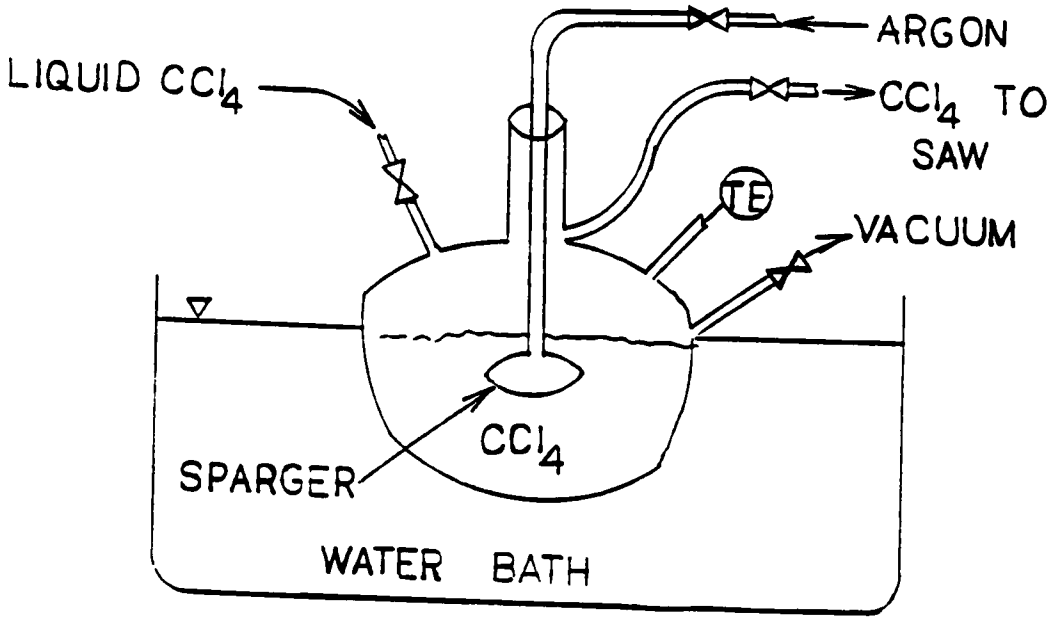

Figure 4.5 Delivery System for Carbon Tetrachloride and Argon

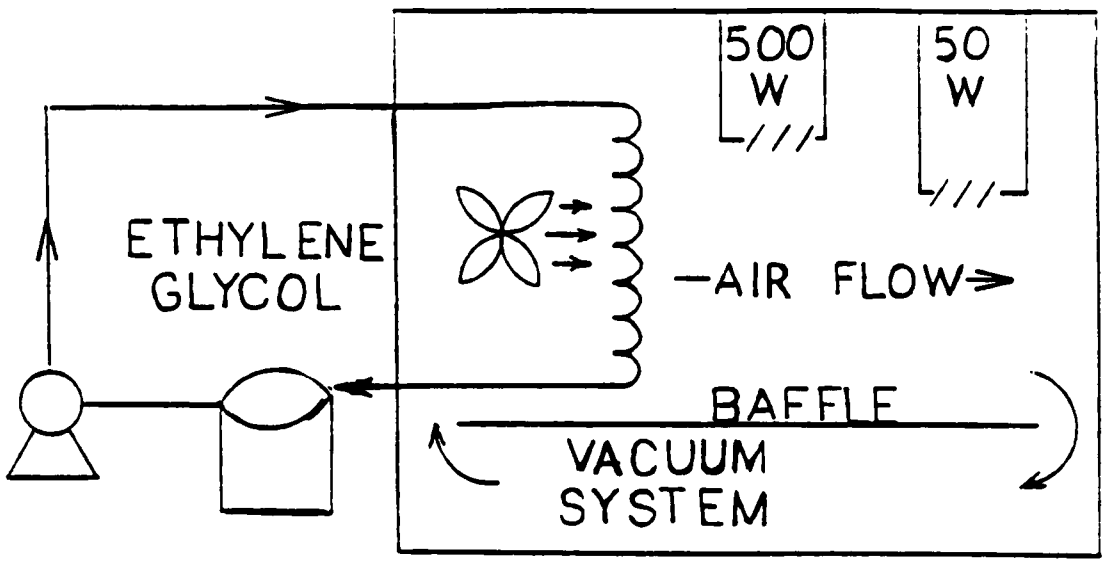

Figure 4.6 Temperature Control System

withstanding high temperatures. Housed within the insulating box were two heaters, a 500-Watt (W), a 50-W heater, and an ethylene glycol cooling mechanism. The 500-W heater was controlled by a Brown 520 solid state control unit and K type thermocouple that roughly controlled the temperature in the box. The cooling system or the 500-W heater remained on constantly while the 50-W heater was used for fine temperature control. A Sargent-Welch thermonitor, model S-82052, with a sensitivity of $\pm$ 0.001°C regulated the 50-W heater in the box through a thermistor placed approximately six inches above the floor of the box in the central area of the vacuum system. A large baffle to which a small fan was mounted was placed approximately two inches above the vacuum system to ensure better circulation of air. A thermocouple placed in the approximate center of the box displayed the temperature of the box to the nearest 0.1°C.

SAW Properties

Figure 3.1 is a general schematic of the two dual delay line SAW devices that were used to measure the frequency shift due to adsorption of mass onto the surface of the SAW devices. Figure 4.2 shows a schematic of the SAW device that was used in this study. The sensitivity and selectivity of the dual delay line SAW apparatus depends on several factors such as the resonant frequency of the SAW, the design of the interdigital electrodes, the number of

electrode pairs, etc. When the frequency output from two SAW devices is mixed, a difference frequency is obtained, which is proportional to the difference in mass adsorbed onto the surface of the SAWs. In principle, pressure and temperature differences that can strongly alter the difference output may be alleviated by using a reference in line SAW device. Some of the properties and physical characteristics of the SAWs used in this apparatus and the design of the entire adsorption measuring system are described in the following paragraphs.

The SAWs (Figure 4.2) were purchased in the described configuration from Microsensor, Inc., located in Fairfax, Virginia. The Microsensor SAW device utilized in the experimental apparatus has a nominal frequency of 112 MHz but is capable of operating at a number of resonant modes in the frequency range of 108 to 116 MHz. The interdigital electrodes were fabricated on ST quartz using gold metallization on top of a thin layer of titanium. The number of fingerpairs was 50, the finger spacing was 7 μm, the finger width was 7 μm, and the acoustic aperture was 23,240 μm. Each chip actually contained two SAW transducers; the overall size of each chip was 1 cm by 1 cm.

Only one of the two SAW transducers on each chip was utilized at each location in the apparatus, and the output frequency from the experimental SAW transducer was mixed with the output frequency of the reference SAW transducer on

the second chip. The change in frequency would be proportional to the mass loading of the adsorbing gas or gases. In other words, mass adsorbed onto the surface of a SAW device causes an attenuation of the device's resonant frequency; this attenuation is a proportional measure of the quantity of mass adsorbed onto the surface (i.e., the more mass adsorbed, the greater the frequency shift). When properly functioning, the present experimental setup corrects for any problems that might result from ambient temperature changes such as changes in the temperature coefficients of delay. Both delay lines on each chip can be used if more surface area for adsorption is needed.

One transducer line, which would be exposed only to a nonadsorbing gas, was labeled as the reference SAW, and the other was labeled as the experimental SAW because it would be exposed to varying partial pressures of adsorbing gas. The frequencies of the two transducers were mixed and amplified to provide a frequency equal to the difference of the two oscillator frequencies (Figure 3.1). The change in frequency due to adsorption is several orders of magnitude smaller than the resonant frequency of each individual SAW. Thus, the difference measurement increases the recordable sensitivity by at least several orders of magnitude. Figures 4.7, 4.8 and 4.9 are diagrams of the electrical

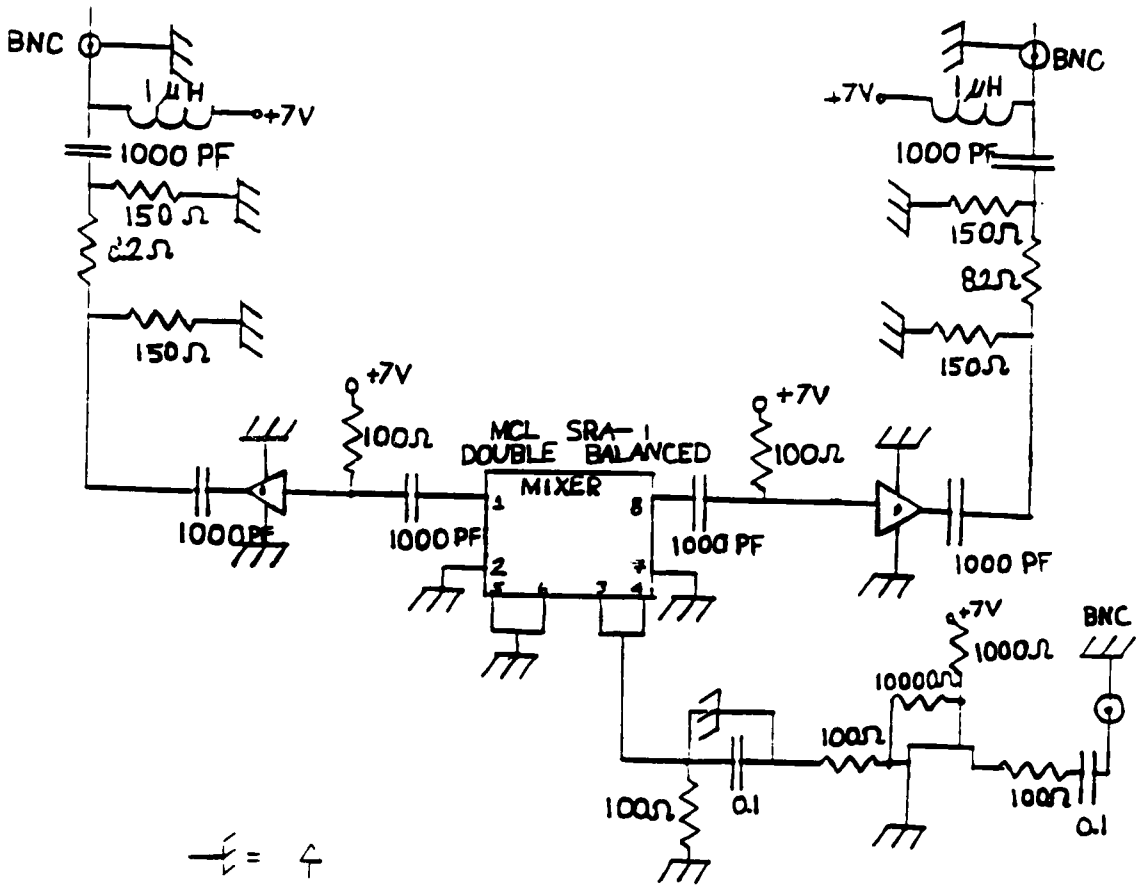

Figure 4.7 Electric Circuitry for SAW Apparatus

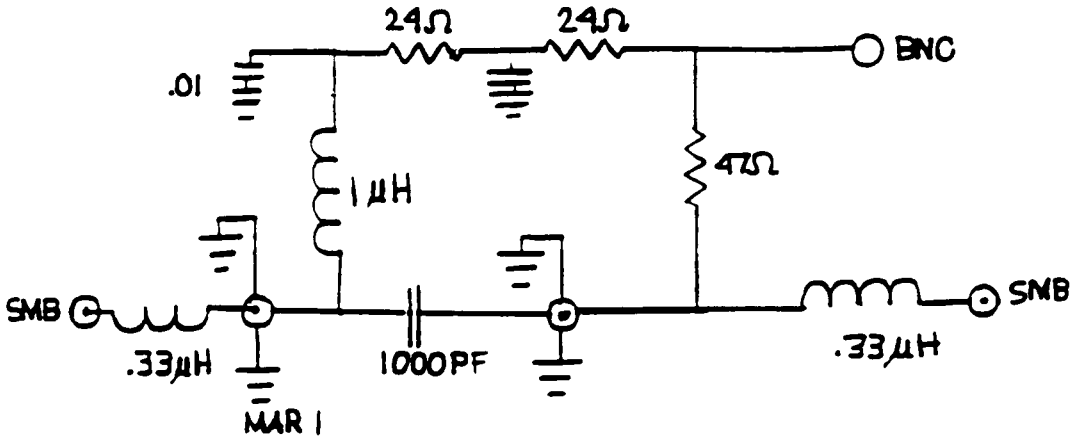

Figure 4.8 Oscillator Circuitry for SAW Apparatus

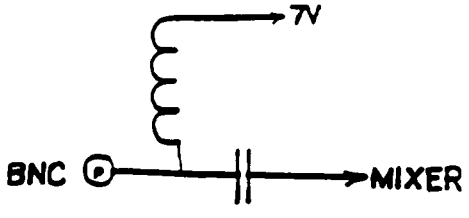

Figure 4.9 Power Supply for SAW Apparatus

circuitry involved in mixing the outputs from the two SAWs and the amplification of the result.

A Hewlett-Packard 5315A/B 10-MHz Universal Counter was used to measure the frequency shift in the apparatus. This instrument is capable of detecting $\pm$ 10 Hz in 1.0 X 10^8 Hz when the period for counting is set at one second.

Cahn Microbalance

A Cahn microbalance, model 2000, (Figure 4.9) manufactured by Cahn, San Angelo, California, was installed to measure the mass of carbon tetrachloride adsorbed on ST quartz. By utilizing known surface area of ST quartz and the resulting weight gain found after the adsorbing gas had flowed through the system, it was possible to determine the adsorbed mass which produced a specific frequency shift in the apparatus. ST quartz was the material of which the SAWs were composed and on which the interdigital electrodes of the SAWs were fabricated; it was also used as the adsorbing medium in the Cahn. The microbalance was connected directly in the experimental side of the vacuum system so that it would be subject to the same pressure, composition, and temperature conditions under which the experimental SAW was maintained (Figure 3.1).

The ST quartz wafers that were used as the adsorbing medium in the Cahn were obtained from V-A Optical Labs, Inc. of San Anselmo, California; they were purchased as 1 by 2.0

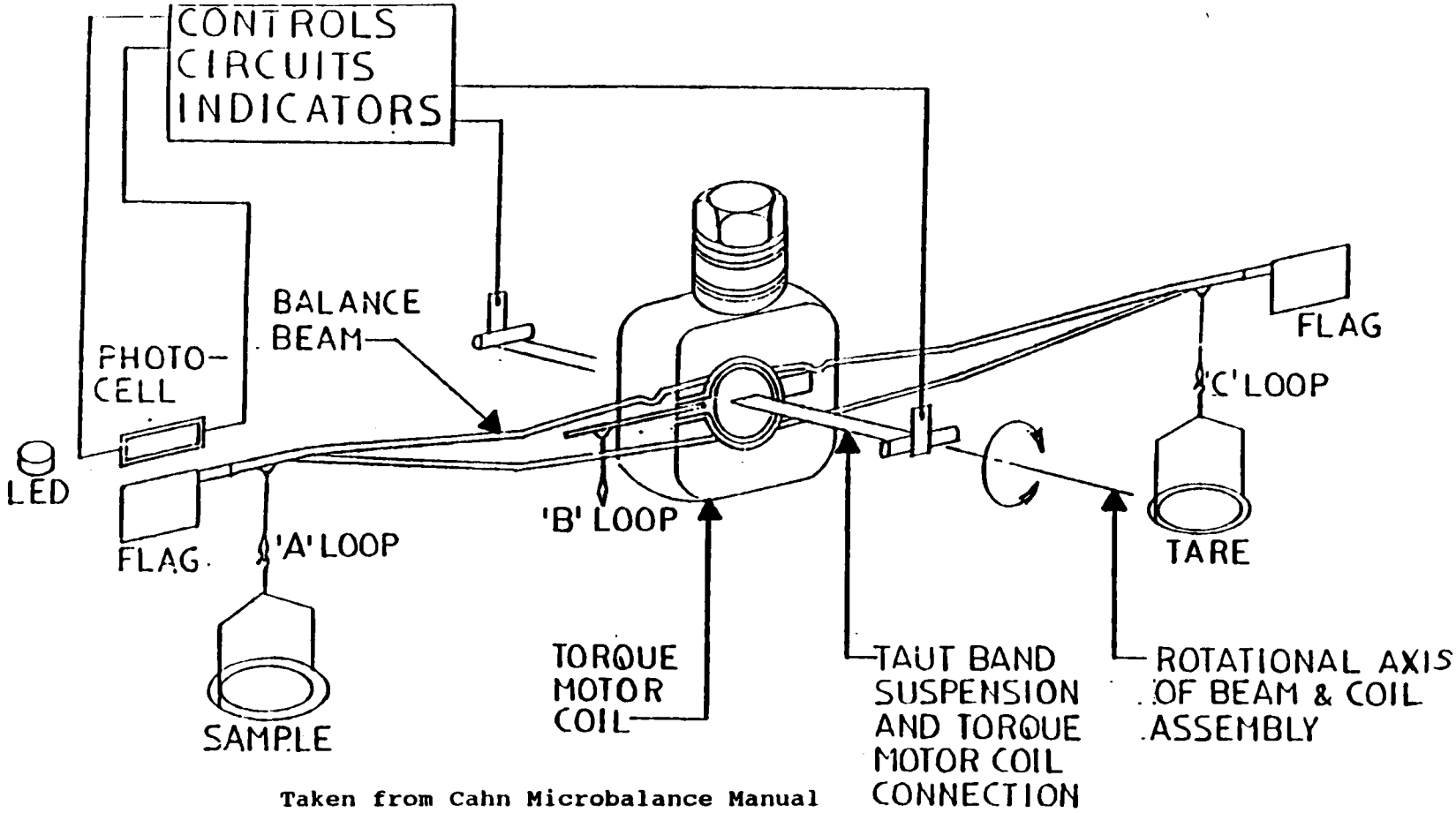

Taken from Cahn Microbalance Manual

Figure 4.10 Cahn Microbalance

by 0.10 inches in size and lapped to a thickness of 0.002-inch, which yielded a total surface area of approximately 79.71 cm^2\wafer. It was calculated that at least 5 wafers were needed to have enough surface area to adsorb a quantifiable mass of carbon tetrachloride. A cube of the same quartz material and equal to the weight of the five wafers was used as the counterweight (Figure 4.9); its surface area was approximately 3.4 cm^2. The mass adsorbed per unit area could be determined precisely, based on the simple relationship on which the Cahn works. (Appendix A illustrates a sample calculation.)

The Cahn 2000 may be described as an electric current-torque transducer (Figure 4.9). It consists of (1) a balance beam mounted to, supported by, and pivoting about the center of a taut ribbon; (2) a torque motor coil located in a permanent magnetic field and also mounted to the taut ribbon; (3) sample suspension fixtures; (4) a beam position sensor system; and (5) controls, circuitry, and indicators. Weights to be measured are applied on one side of the beam with known counterweights applied to the opposite side. The forces acting from both sides of the beam produce a torque about the axis of rotation as do the electric current flowing in the torque motor coil and the taut ribbon. When the beam is at its horizontal reference position and when the torque from the torque motor equals the sum of the torques from the taut ribbons and from the weights on the

beams, the beam is balanced. At the balanced position, the electric current flowing in the torque motorcoil is a direct measure of the forces applied from the beam and the taut ribbon. The Cahn 2000 is sensitive to weight changes as small as 0.1 μg. However, mechanical vibrations from external sources can adversely affect its capabilities to monitor mass changes at this range.

The microbalance, as received from the previous user, was expected to be able to achieve pressures as low as 1.0×10^{-7} torr. Several modifications had to be made to the balance before these pressures were attainable with the vacuum system that housed the Cahn. The original plastic coatings on the wiring of the balance degassed badly under high and ultra high vacuum conditions. All wiring was removed from portions of the weighing mechanism that would be located inside the vacuum system. This wiring was stripped and then insulated by ceramic beads to alleviate degassing. The removal of the plastics removed an adsorbing contaminant gas that would have been adsorbed onto the SAWs or quartz wafers and would have been incorrectly incorporated into the calibration of mass versus frequency shift. The modifications made in no way affected the sensitivity or working mechanisms of the balance.

The microbalance was secured by means of a spring mechanism in a 6-inch SS cross. This setup provided a means of leveling the Cahn and allowing the quartz wafers and

quartz cube to be freely suspended within the hangdown tubes (area for sample suspension) of the Cahn. The cross was directly attached to the experimental side of the vacuum system where it was subjected to the same conditions as the rest of the apparatus. The microbalance could be easily separated from the vacuum system by disconnecting two flanges and inserting a blank flange into the vacuum system.

The Cahn microbalance will be discussed further in the Results and Discussion section.

4.1.2 Procedure

Initially the components of the UHV system that are able to be baked were heated to approximately 450°C until no further increase in system pressure was noted or until a subsequent slight decrease in system pressure was noted. This time varied depending on the cleanliness of the system but typically took two to three days. All valves in the UHV system except the inlet valves were fully opened during bakeout. The system was subsequently pumped down overnight to its ultimate attainable vacuum. This procedure (or a modified procedure that utilized bakeout temperature of 100 to 150°C) was followed each time the system was opened to the atmosphere or carbon tetrachloride was admitted to the system.

The original plan was to obtain data on frequency shift versus pressure at three temperatures: 16°C, 24°C

(ambient), and 45°C. However, the air bath temperature control system was unable to maintain constant uniform temperature throughout the box at set points very different from ambient. Therefore, initial experiments were conducted at or near ambient temperature to illustrate feasibility of the apparatus.

The initial experiments were to involve a pure adsorbing gas at low pressure. For these experiments, valves L1 and R1 (Figure 4.3) were closed to force gas flow through the two GP valves. The tee valve connecting the turbomolecular pump and the two sides of the vacuum system was also closed. No further changes in the system were made until the system pressure remained constant. At this time the initial frequency difference between the two SAWs was recorded along with the system temperature, carbon tetrachloride, temperature, and the pressure readings from both the reference and experimental sides of the vacuum system.

Carbon tetrachloride, HPLC grade, obtained from J. T. Baker was maintained at 24°C by means of a laboratory water bath. The carbon tetrachloride was transferred into the flask (Figure 4.4), the proper temperature was obtained, and the vapor above the liquid was pumped away to ensure removal of water vapor and other impurities. Valve V1 was opened slowly until a two percent increase in pressure was noted. Valve V2, connected to a supply of mass spectrophotometer-

analyzed argon, was opened to cause an equal pressure increase in the reference side of the apparatus. Frequency difference was monitored every 0.5 sec and recorded every 20 sec. When no further changes in frequency shifts were noted, the experiment was to be stopped.

The Cahn microbalance was used to measure the quantity of mass adsorbed onto the surface of the ST quartz and to correlate that quantity to a particular frequency shift obtained under specific conditions of temperature and total pressure. Prior to gas flow into the system, the quartz wafers and counterweights were cleaned with a solution of ammonium hydroxide and dried. The wafers and counterweights were balanced to within 1 μg to obtain a weight change output of zero from the microbalance. The Cahn and all weights and counterweights located in the vacuum system were baked at 450°C along with the rest of the vacuum system. No further precautions or preparations were made before the carbon tetrachloride was admitted to the system. The final quantity of mass adsorbed onto the quartz plates would be recorded as the mass present when no further changes in frequency shifts were observed. Operational procedures for the Cahn microbalance were supplied from the company and followed strictly. The modifications made to the balance to alleviate degassing did not affect procedures for operating the balance.

Subsequent experiments were conducted with initially higher partial pressures of carbon tetrachloride and greater flowrates of argon. A series of data points recording frequency difference versus partial pressure of carbon tetrachloride was to be obtained from UHV conditions to atmospheric conditions.

Throughout all experimental trials, we were unable to maintain stable frequency output from the SAW devices and were not able to zero the Cahn microbalance at its greatest sensitivity level. These problems are discussed in the next chapter.

CHAPTER 5.0

RESULTS AND DISCUSSION

Initial results from the SAW apparatus for measuring adsorption were unreliable.

The major problem encountered was an inability to maintain a stable resonant frequency. Initially, it was considered that the difficulty might be due to nonuniform temperatures around the SAW devices. To correct this problem the temperature control system was shut down, and the system was allowed to cool to ambient temperature. The temperature control box was closed so that drafts would not cause temperature inconsistencies between the two SAW devices. Still, a stable frequency difference could not be maintained when the system pressure was as low as 5.4×10^{-8} torr, and no gases were being transferred into the vacuum system. One SAW device drifted $+57 \times 10^{3}$ Hz (at ca. 102×10^{6} Hz) in a four minute period,and the other drifted $+ 12 \times 10^{3}$ Hz (at a ca. 100×10^{6} Hz) during the same period. Under conditions of proper operation each SAW device should have maintained a stable resonant frequency to within 10^{1} to 10^{2} Hz for hours. Therefore the frequency difference was unstable. There was constant fluctuation in

these ranges. The frequency counter displayed inconsistent resonant frequencies from day to day even though no changes were made in the system.

Because maintenance of a stable resonant frequency with either SAW device or a stable frequency difference was not possible, it was decided to leak argon into one side of the apparatus to determine whether any trend in frequency difference would develop. According to theory, increasing the pressure on one of the SAW devices should have caused an attenuation in the surface waves, and thus, have created a greater frequency difference between the experimental and reference SAW devices. However, this did not occur. Figures 5.1 through 5.4 illustrate the frequency difference versus pressure for ranges from 2.0×10^{-7} to 8.4×10^{-4} torr. In all plots, argon gas was the source of increasing pressure. The frequency differences were expected to remain relatively constant because pressures on both sides of the system were increased by identical flow rates of argon. However, this did not occur.

Figure 5.1 shows a frequency difference shift from 1.7236×10^{6} Hz to 1.5×10^{6} Hz over a period of five minutes for a constant pressure of 3.4×10^{-7} torr. As the pressure was increased, the frequency differences did not increase at the same rates as they had initially. Figures 5.2, 5.3, and 5.4 show lesser frequency difference changes for greater total pressure changes. There is also little consistency in

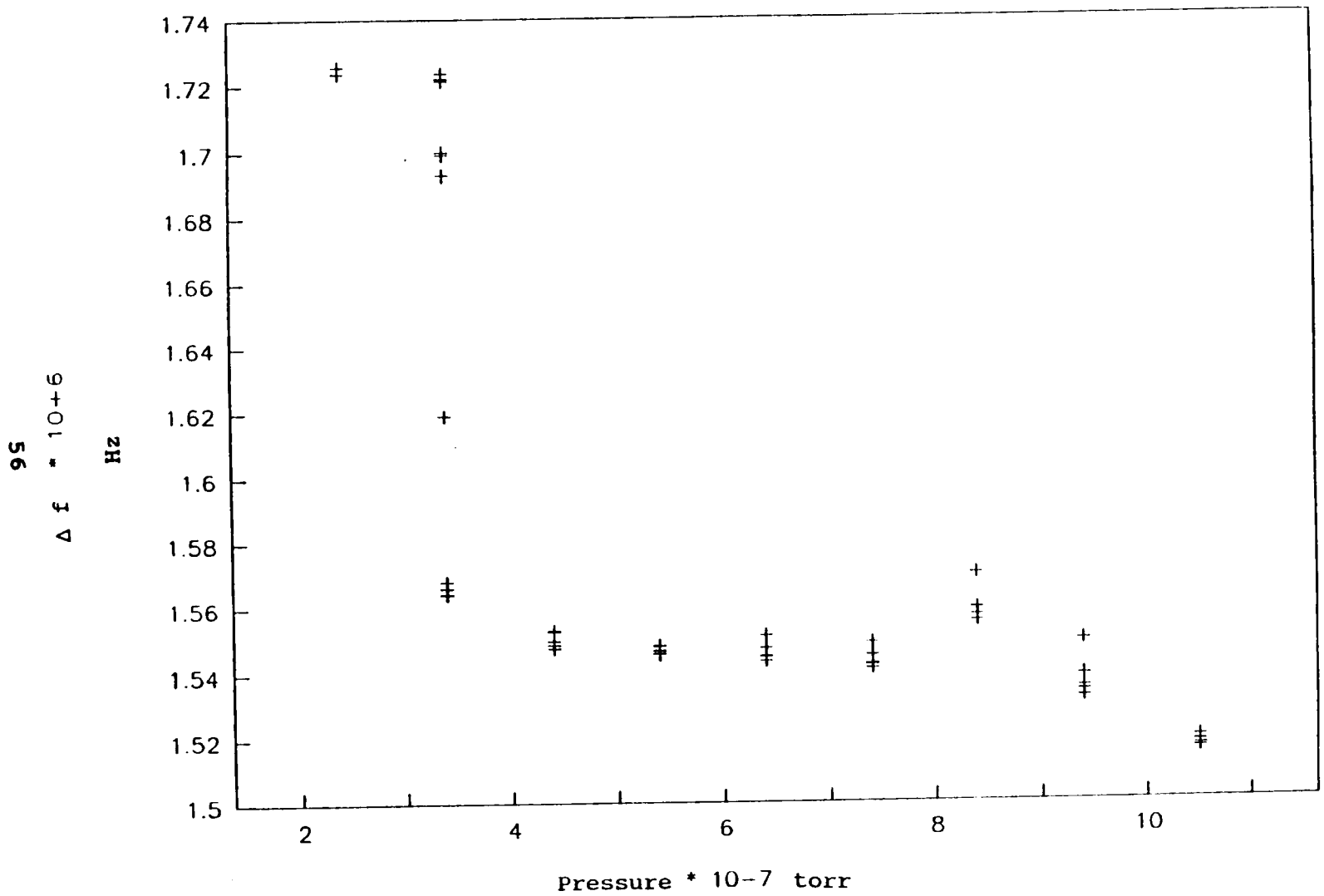

Figure 5.1 Frequency Difference vs,. Pressure of Argon at 10^{-7}

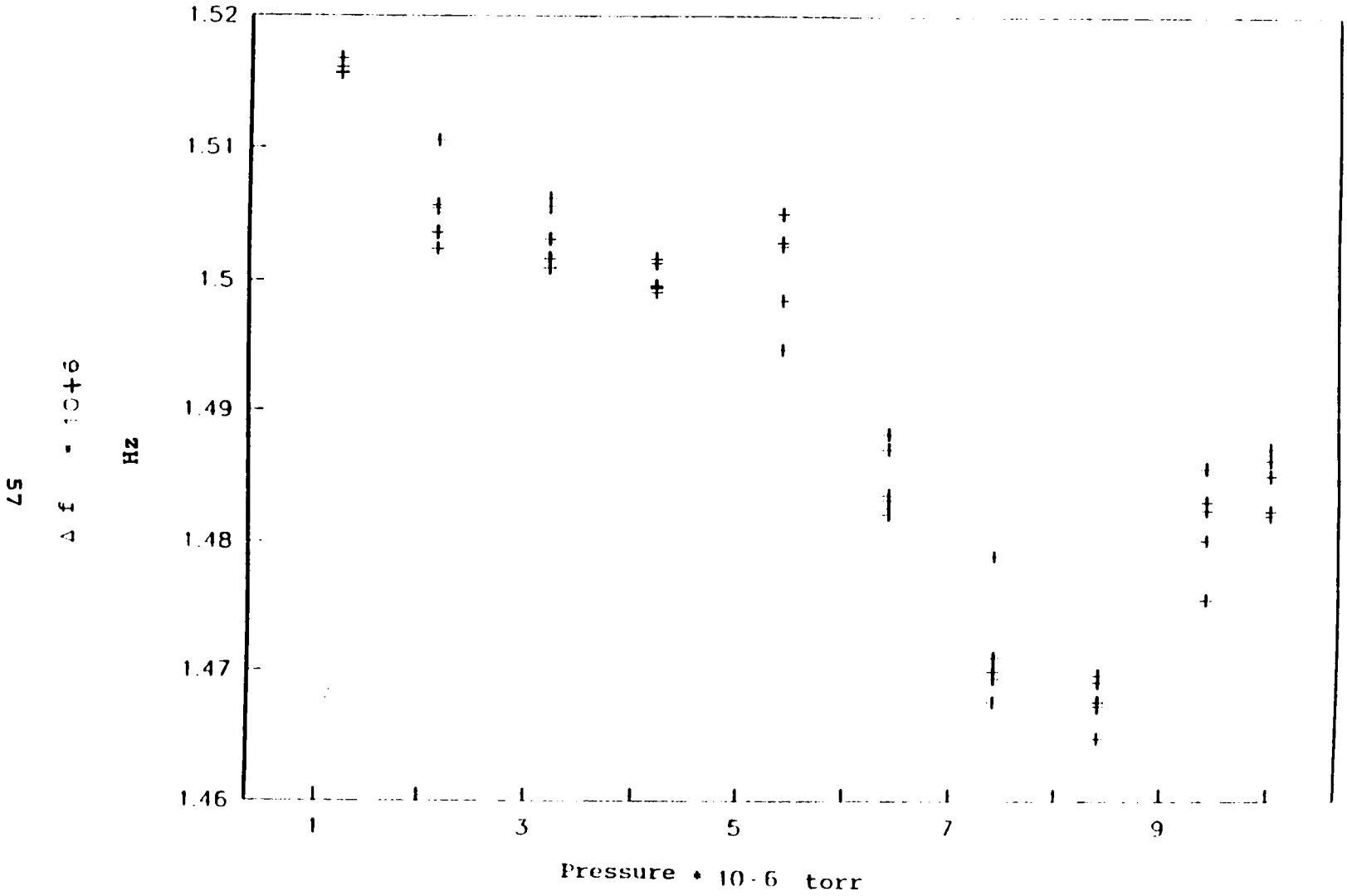

Figure 5.2 Frequency Difference vs,. Pressure of Argon at 10^{-6}

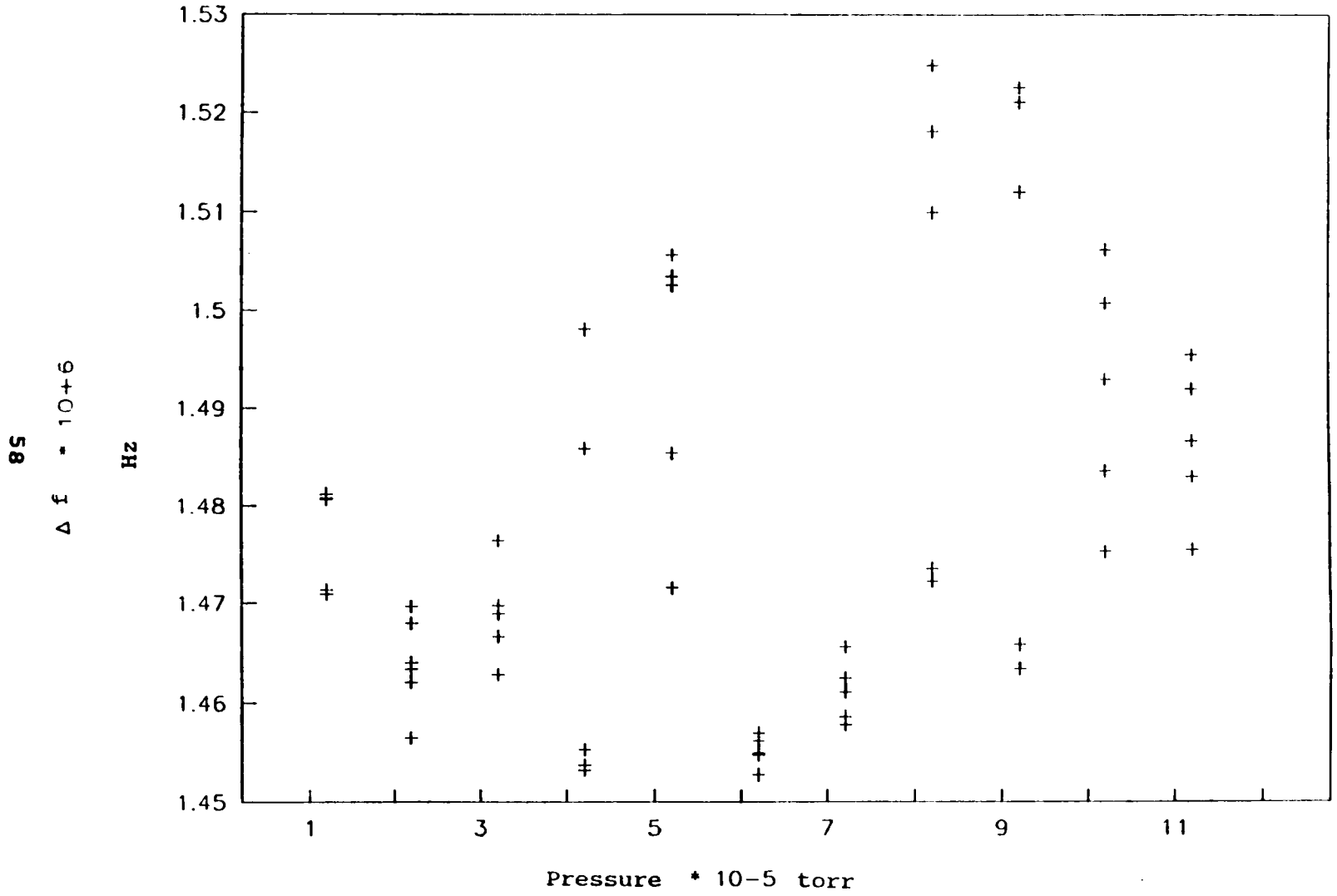

Figure 5.3 Frequency Difference vs,. Pressure of Argon at 10^{-5}

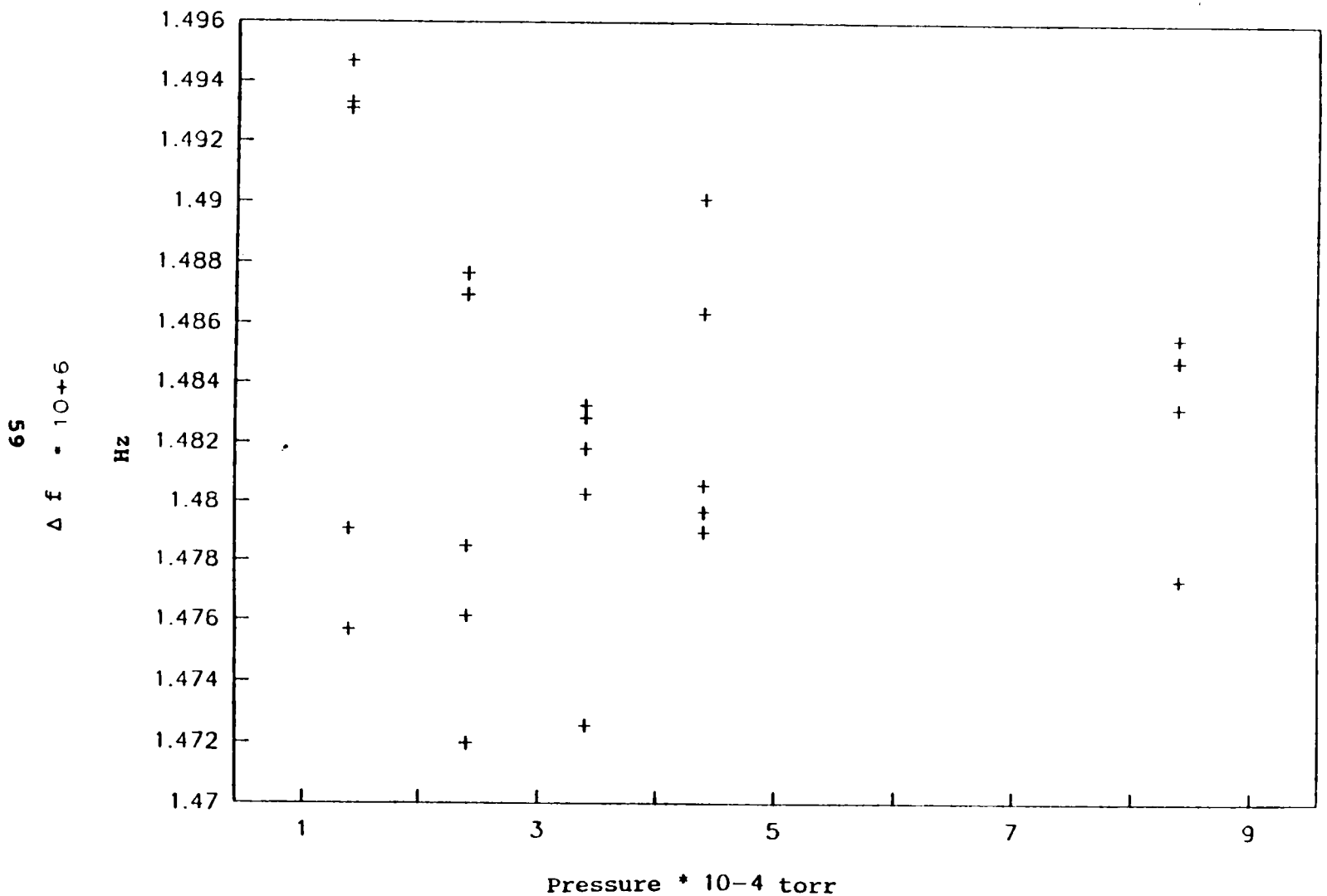

Figure 5.4 Frequency Difference vs,. Pressure of Argon at 10^{-4}

the Δf in a particular pressure regime. Figure 5.5, a plot of log of pressure versus frequency difference, shows more clearly that the same frequency differences exist throughout all pressure regimes.

The next experimental trial involved admitting carbon-tetrachloride to the experimental side and argon onto the reference side of the apparatus. Initial conditions showed a pressure of 1.0×10^{-5} torr, a Δf of 1.5178×10^{6} Hz, a system temperature of 27°C, and a partial pressure of approximately 100 mm of Hg in the flask of liquid CCl_4. Figure 5.6 shows a plot of the data obtained during this experiment. As the partial pressure of CCl_4 increased on the experimental side, the frequency difference should have increased; instead, the opposite effect was seen. After these results were observed, the experimental side was entirely opened to the flask of CCl_4; no change in Δf was observed.

It was concluded that the SAW devices were not functioning properly or temperature differences had a greater effect than was expected.

Nude thermocouples were attached to flange containing each SAW device and connected so that a voltage difference, indicating a temperature difference, could be monitored. Figure 5.7 is a plot of frequency difference versus the voltage doe to temperature difference in the two SAW devices. Again, the results of this trial were the opposite

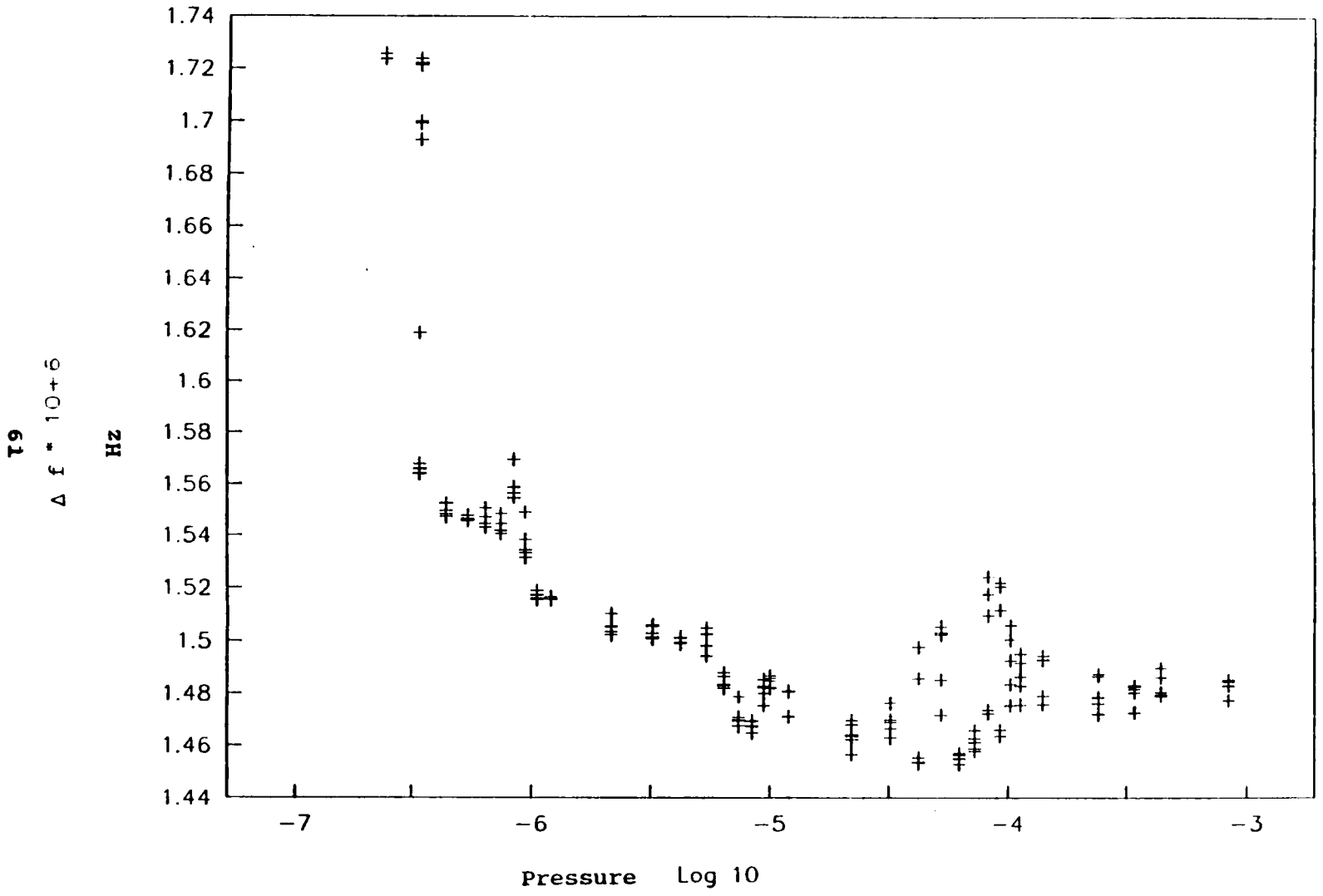

Figure 5.5 Frequency Difference vs. Pressure for Ar/CCl_4

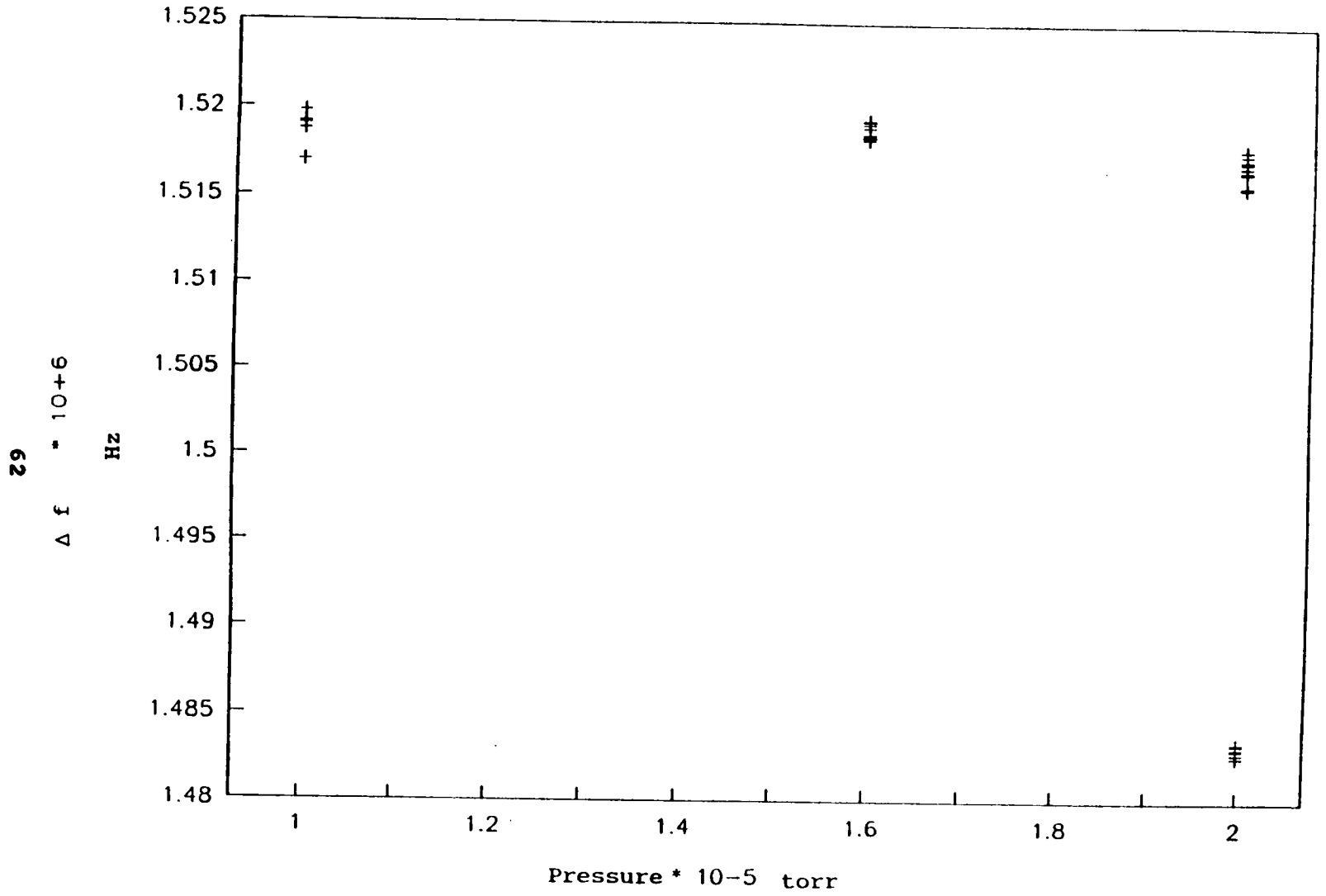

Figure 5.6 Frequency Difference vs. Pressure of CCl_4

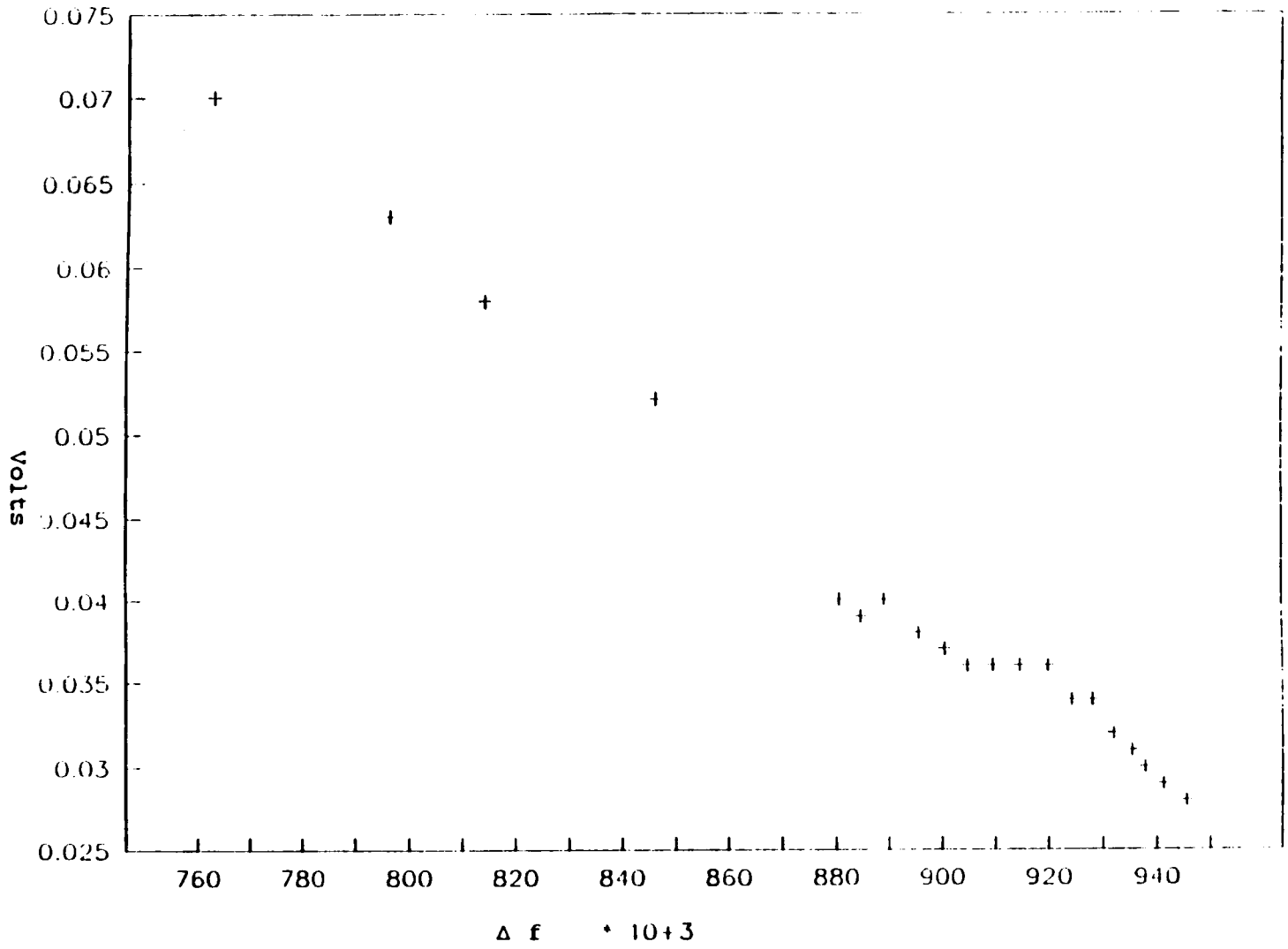

Figure 5.7 Frequency Difference vs. Temperature Difference Measured in Volts

of what was expected; as the temperature difference increased, as shown by a greater voltage difference, the frequency difference decreased.

The system was left overnight with all conditions unchanged to see if the temperature would stabilize. Figure 5.8 is a plot of the frequency difference versus the voltage due to temperature difference after a fifteen hour stabilization period. Readings were taken every thirty minutes; the order of the temperature and frequency differences are indicated on the plot. Again, there is no consistency in the data. It should also be noted that the frequency differences are in the 10^3 range rather than in the 10^6 range where all previous experimental data were taken. The only explanation for this sudden change in the range of frequency differences is that the SAW device electronics or the device itself malfunctioned.

The nude thermocouples, wired in a delta configuration, were then placed into a distilled water ice bath so that the reference point for temperature measurement would confidently be 0°C. The temperature control box was set to a temperature of 35.22°C and left for several hours before data were taken. Figure 5.9 shows the results of Δf versus ΔT (as measured by voltage difference). Again, temperature and frequency differences exist, as was expected; however, the frequency differences increase as the temperature differences decrease. This plot does not show the shift in

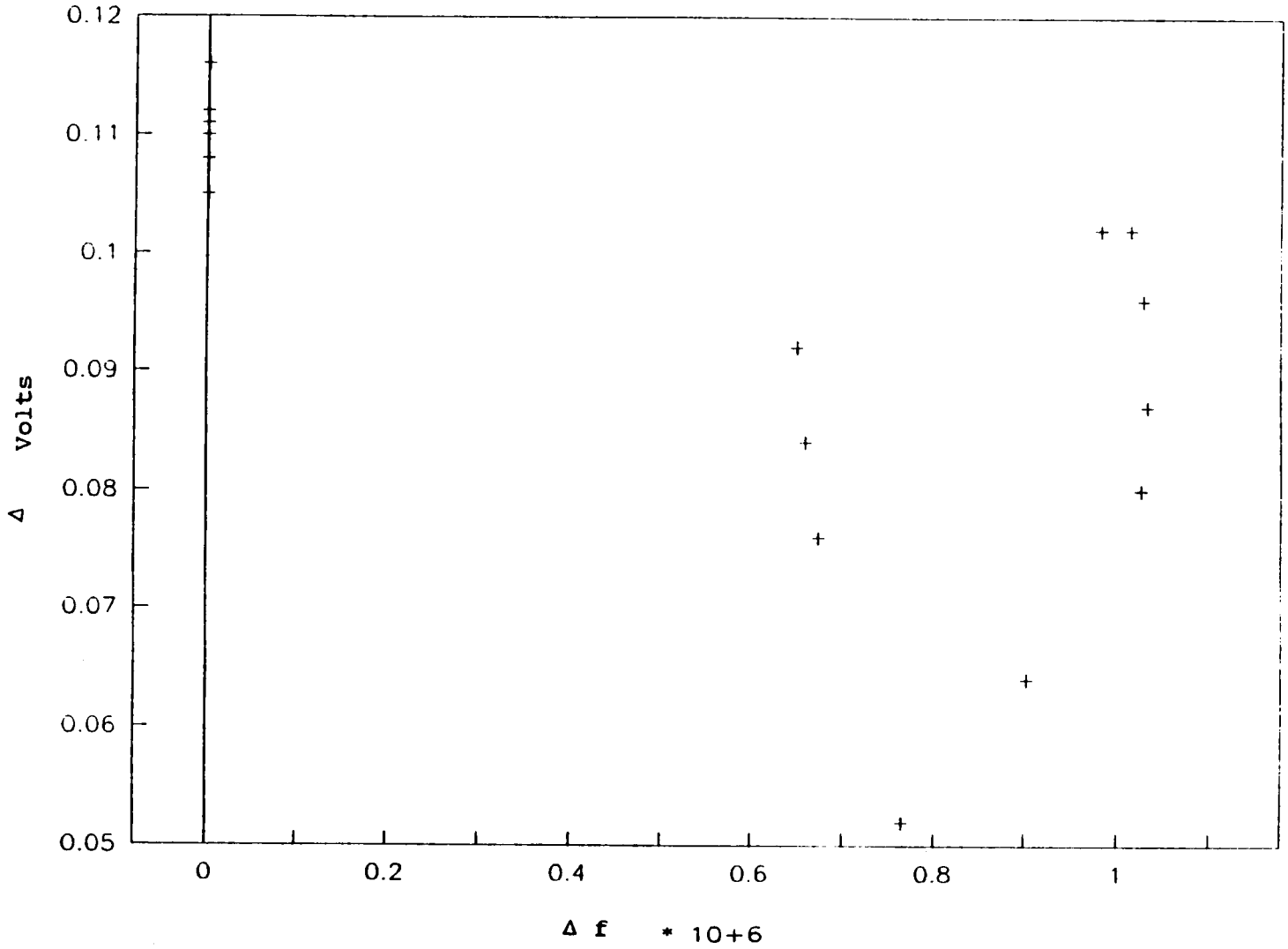

Figure 5.8 **Frequency Difference vs. Temperature Difference Measured in Volts**

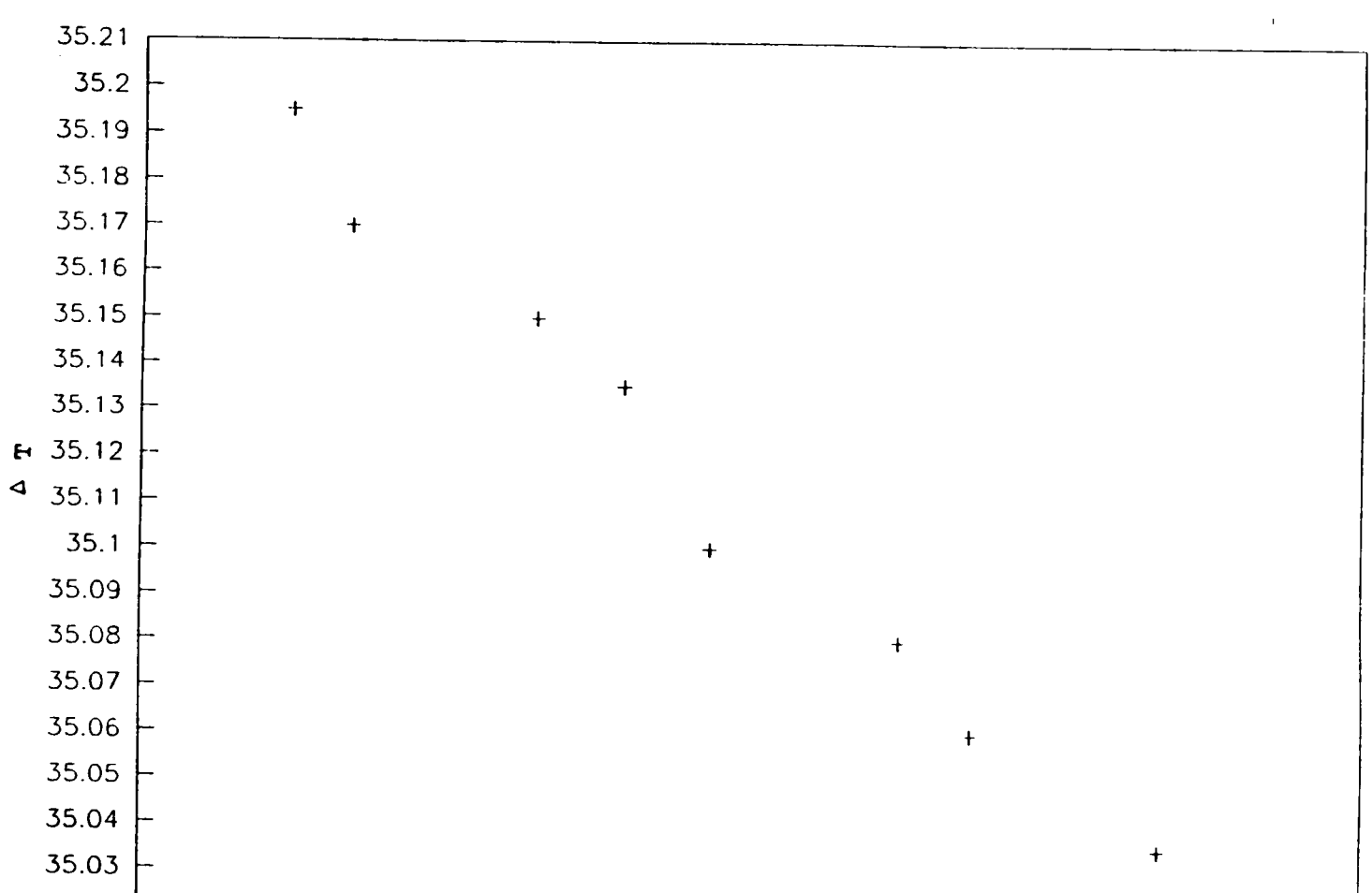

Figure 5.9 Temperature vs. Frequency Difference

Δf from the 10^3 Hz range to the 10^6 range; the raw data including the 10^6 range data may be seen in Appendix B. The results of this experiment confirm that the SAW devices and their electronics were not functioning properly and that temperature control within the box was insufficient.

Upon removing the SAW devices from the vacuum system, it was discovered that the electrodes were damaged due to metallic sputtering. It was first assumed that the ultra-high vacuum ionization gauges had in some way caused the thorium-iridium filaments to sputter onto the SAW devices. This was not the case.

The damaged SAW devices were replaced with new SAW devices. Again, no stable frequency was obtained even though the difference frequency was much more stable than in previous trials. Stability to 1000 Hz was obtained for the difference frequency and the individual SAW devices. After leaving the system, under ultra-high and high vacuum conditions, to stabilize for several days it was discovered that the stability could no longer be obtained. Again, the SAW devices were examined and it was determined that the electrodes were severely damaged. The reason for this damage could have resulted from ion bombardment resulting from ionization of atmospheric gas that leaked into the system caused by the radio frequency high voltages imposed on the SAW devices. Raw data for the last trials may be seen in Appendix B.

The Cahn microbalance could not be zeroed or tarred at the proper point due to mechanical vibrations present in the vacuum system. Stability was obtained to a degree that allowed measurement of mass in the tenths of milligram range, but never at greater precision. This prevented the development of a frequency shift versus mass adsorbed correlation even if the SAW device apparatus had proved successful.

Various attempts were made to reduce or alleviate the mechanical vibrations caused, primarily, by the roughing pump: (1) The original pump was exchanged for one that was designated as having extremely low vibrations (<2 Hz), (2) vibration isolation adsorbers (neoprene rings) were added to the walls of the merinite box to which the housing of the Cahn was attached, (3) the stand and merinite box housing the vacuum apparatus was placed on foam pads so that vibrations due to movements in the room would be adsorbed to some extent. None of these measures alleviated mechanical vibrations enough that the Cahn could be tarred and used to measure microgram weight changes.

CHAPTER 6.0

CONCLUSIONS AND RECOMMENDATIONS

6.1 Conclusions

Although the objectives of the study were not met, valuable information was gained from the initial trials. No firm conclusions may be drawn from this investigation, but with implementation of the recommendations that follow, the feasibility of the SAW device as a means to measure equilibrium and dynamic adsorption may be tested, which may yield more conclusive results.

6.2 Recommendations

The experimental apparatus as described in this paper did not allow the frequency difference versus pressure to be measured. There are several reasons for not attaining the original experimental objectives. The following recommendations would greatly increase the likelihood of meeting the objectives.

1) Apparatus design

The apparatus should have been designed as two separate systems: one for the adsorbing gas and one for the nonadsorbing gas. A common pressure/flow control

system should be central to both systems. A schematic of the proposed design may be seen in Figure 6.1.

2) Pressure/flow control

The pressure-sensing devices should have the capability of automatically controlling the GP control valves to a much greater degree of precision than they were capable of doing with the present arrangement. Two different pressure-sensing systems should be used, one for lower pressure (in the range of 1.0×10^{-7} to 1.0×10^{-3} torr) and a second control mechanism for pressures in the range of 1.0×10^{-3} torr to atmospheric pressure. The DC output from the Varian UHV pressure gauges could be connected to the electronics units controlling the GP valves, which would allow for much greater total pressure control in the lower pressure regions than was managed by the manual pressure control mechanism. The GP valves are capable of controlling pressures from atmospheric down to 1.0×10^{-11} torr. When system pressures exceeding 1.0×10^{-4} torr are reached, the UHV control would be switched to either millitorr gauges (control would be through the same mechanism as for the UHV gauges) or MKS pressure-sensing heads as used in the present system.

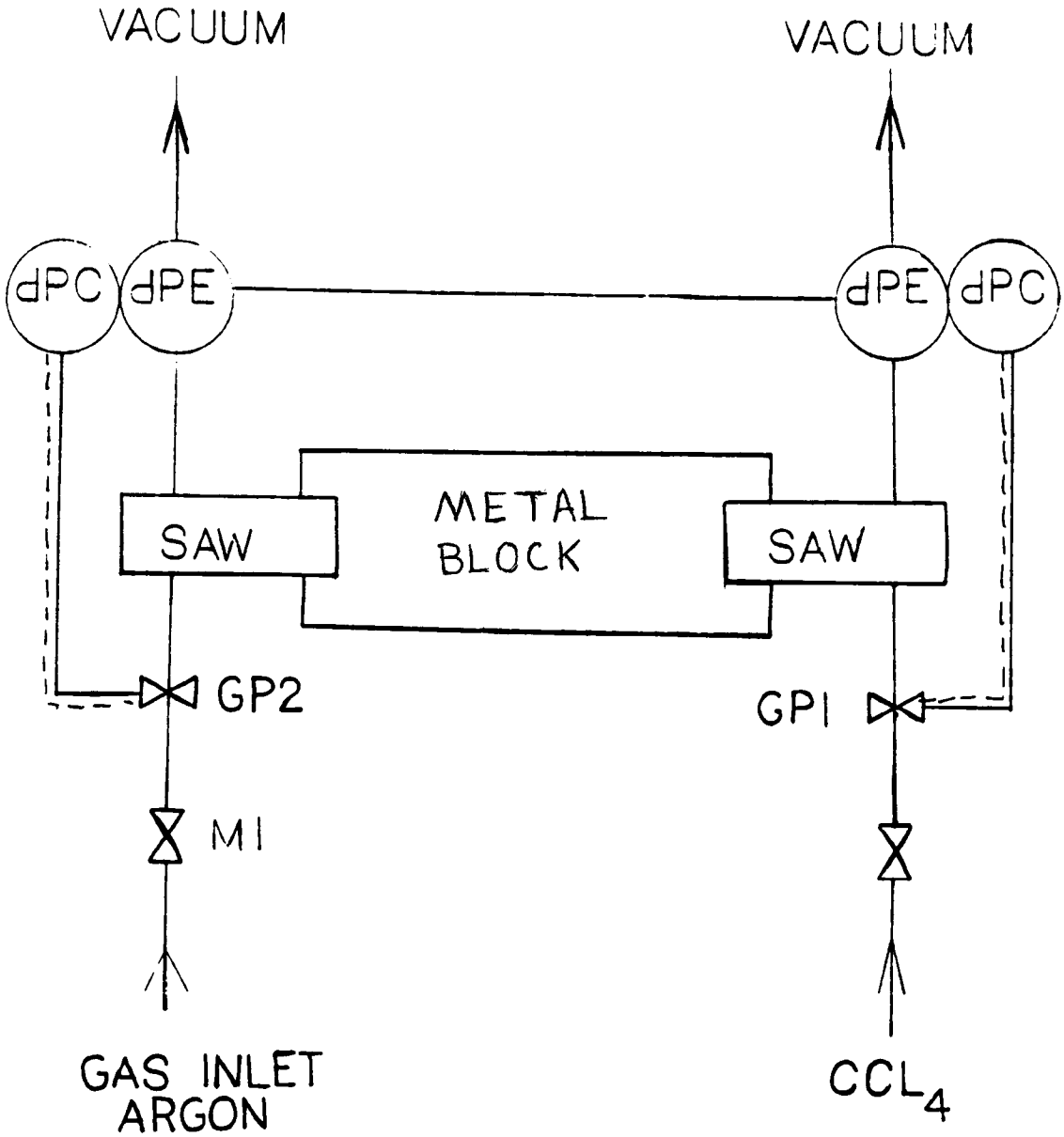

Figure 6.1 Schematic of Proposed SAW Apparatus Design

3) Reduction of Vibrations

Facilities for reducing vibration in the system should have been included in the design of the system to alleviate mechanical vibrations that caused instabilities in the 10- and 1000-torr MKS sensor heads and the Cahn microbalance. Due to limited laboratory space, the entire vacuum apparatus was built in an area that allowed mechanical vibrations to be transferred through the floor of the laboratory to the microbalance and to the pressure-sensing devices which were operated by movement of a thin diaphragm. Attempts were made to correct the vibration problem by mounting the devices with neoprene absorbers and using a roughing pump which should not transfer vibrations to the pressure sensing devices. These corrective actions did not sufficiently alleviate the problem; it is believed a large vibration adsorber located underneath the entire vapor sensing device would eliminate the problem.

4) Temperature control

A better method of temperature control is needed because the transducers are extremely sensitive to temperatures immediately surrounding their surface. It has been demonstrated that maintenance of a temperature difference less than one degree between the two SAW

transducers is impossible with the current air bath system. Two SAW transducers should be mounted very close to each other on a common metal block, such as copper, which has good heat transfer properties. A thermocouple should be inserted into the metal block to ensure accurate temperature control. By this mechanism, stringent temperature control around other parts of the apparatus would be unnecessary. As long as temperatures surrounding the apparatus are kept sightly higher than the temperature of the block, no problems should arise.

5) Mass spectrometer

The attachment of a mass spectrometer for residual gas analysis onto each system would ensure proper cleanliness of the system before adsorption studies utilizing the SAWs began and could be a great aid in determining the extent to which adsorption was occurring in a given time period.

6) Ionization gauges and controllers

New ionization gauge controllers should be purchased and used to ensure dependable total system pressure. Many times, after a shutdown of the apparatus, it would take days to conclude that the gauge controllers were or were not working properly. If the UHV gauges are to

be used to control the operation of the GP valves and thus the total system pressure, it is imperative that they function properly and reproducibly.

7) SAW IDT Electrodes

Stability of the resonant frequencies of each SAW device was unattainable even after attempts to stringently control the temperature of the surrounding environment. It was twice observed that the IDT electrodes on the SAW transducers became damaged by ion bombardment. This could have been caused by background gas being ionized by radio frequency high voltage. After discussing the problem with electronic experts, no recommendation can be made at the present time which might alleviate the electrode damage problem which occurs under high vacuum conditions.

LIST OF REFERENCES

LIST OF REFERENCES

1. Auld, B. A., Acoustic Fields and Waves in Solids, Vol. 2, Wiley-Interscience, New York, 1973.

2. Bryant, A., D. C. Lee and J. F. Velelino, "A surface acoustic waves detector", Proc. IEEE Ultrasonics Symp.,IEEE Elec Cat 81CH1689-9 (1981) 1735-1738.

3. Bryant, A., M. Poirier, G. Riley, D.L. Lee and J. Velelino, "Gas Detection Using Surface Acoustic Wave Delay Lines", Sensors and Actuators, 4(1983) 105-111.

4. Carberry, J. J., and A. Verma, Chemical Reactions and Reactor Engineering, Marcel Dekker, New York, 1987, 151-238.

5. Chuang, C. T., R. M. White and J. J. Bernstein, "A thin membrane surface acoustic wave vapor sensing device", IEEE. Dev. Lett. EDL-3 (1982) 145-147.

6. D'Amico, A., A. Palmer, and E. Verona, "Surface Acoustic Wave Hydrogen Sensor, Sensors and Actuators 3(1982/83) 31-39.

7. Dyke, K. S., U. S. Patent 257, 171 (July 4, 1945).

8. Flynn, T. M., H. Hinnah, D. E. Newell, "Improved Cryogenic Thermometer," paper F-2, 1962 Cryogenic Engineering Conference, L. A., Calif.1962.

9. Guilbault, G. G., J. Affolter, and Y. Tomita, "Piezoelectric Crystal Coating for Detection of Organophosphorus Compounds", Anal. Chem., 53(1981) 2057-2060.

10. Ho, H. and G. Guilbault, "Continuous Detection of Toluene in Ambient Air with a Coated Piezoelectric Crystal", Anal. Chem. 52(1980) 1489-1492.

11. King, W. H. Jr., "Piezoelectric Sorption Detector", Anal. Chem., 36(1964) 1735-1739.

12. Kino, G. S., Acoustic Waves: Devices, Imagery, And Analog Signal Processing, Prentice-Hall, Inc., New Jersey, 1989.

13. Konstantinov, A., A. Neubrand, and P. Hess, "Surface Acoustic Waves in Solid-State Investigations",

14. Lewis, M. F., "Surface Acoustic Wave Devices and Applications", Ultrasonics, 5(1974) 115-123.

15. Maines, J. D., E. G. Pagie, A. F. Sounders and A. S. Young, "Simple Techniques for the Accurate Determination of Delaytime variations in Acoustic Surface Wave Structures", Electronics Letters, 5(1969) 678.

16. Mason and W. Perry, Piezoelectric Crystals and Their Application to Ultrasonics, Van Nostrand, New York, 1954.

17. Sauerbrey, G., "Verwendung von Schwingquarzen en zur Wägung dunner Schichten und zur Mikrowägung" Z. Phys, 155(1959) 206-222.

18. Slutsky, L. J. and W. H. Wade, "Adsorption of Gases on Quartz Single Crystals", J. of Chem. Phy, 36(1962) 2688-2692.

19. Wohltjen, H. "Mechanism of Operation and Design Considerations for Surface Acoustic Wave Device Vapour Sensors", Sensor Actuators, 5(1984) 307-325.

20. Wohltjen, H. and R. Dessy, "Surface Acoustic Wave Probes for Chemical Analysis II. Gas Chromatography Detector", Anal. Chem. 51(1979) 1465-1470.

APPENDIXES

APPENDIX A

SAMPLE CALCULATION

1 refers to wafers of ST quartz
2 refers to cube of ST quartz

A_1 = 79.71 cm_2/wafer x 5 wafers = 398.55 cm^2
A_2 = 3.4 cm^2

From the principal of operation of the Cahn, when the forces on the taut ribbon are equal, the Cahn is balanced. A relationship therefore exists between the two sides of the Cahn as such:

$A_1n = N_1$ $\qquad$ $A_2n = N_2$

$N_1 - N_2$ = measured quantity on Cahn
$A_1\ n - A_2\ n$ = measured quantity on Cahn
A_1/A_2 = 117.22

$A_1n - A_2n$ = measured quantity, for example 0.02 μg
117.22 A_2 n - A_2 n = 0.02 μg
116.22 A_2 n = 0.02 μg
116.22 x 3.4 cm^2 n = 0.02 μg
395.15 cm_2 n = 0.02 μg
n = 5.06 x 10^{-5} $\mu g/cm^2$

APPENDIX B

PRESSURE 1

2.4 1.7236	2.4 1.7236
2.4 1.7258	2.4 1.7258
3.4 1.7237	3.4 1.7237
3.4 1.7218	3.4 1.7218
3.4 1.7221	3.4 1.7221
3.4 1.7213	3.4 1.7213
3.4 1.699188	3.4 1.699188
3.4 1.70	3.4 1.7
3.4 1.693	3.4 1.693
3.4 1.6190	3.4 1.619
3.4 1.5643186	3.4 1.564318
3.4 1.565885	3.4 1.565885
3.4 1.56408	3.4 1.56408
3.4 1.566	3.4 1.566
3.4 1.568	3.4 1.568
3.4 1.566	3.4 1.566
4.4 1.5473	4.4 1.5473
4.4 1.5496	4.4 1.5496
4.4 1.5484	4.4 1.5484
4.4 1.5528	4.4 1.5528
4.4 1.5524	4.4 1.5524
5.4 1.5455	5.4 1.5455
5.4 1.5479	5.4 1.5479
5.4 1.5467	5.4 1.5467
5.4 1.5481	5.4 1.5481
5.4 1.5463	5.4 1.5463
5.4 1.5458	5.4 1.5458
6.4 1.5446	6.4 1.5446
6.4 1.5472	6.4 1.5472
6.4 1.5447	6.4 1.5447
6.4 1.5508	6.4 1.5508
6.4 1.5447	6.4 1.5447
6.4 1.5433	6.4 1.5433
7.4 1.5420	7.4 1.542
7.4 1.5409	7.4 1.5409
7.4 1.5422	7.4 1.5422
7.4 1.5448	7.4 1.5448
7.4 1.5486	7.4 1.5486
8.4 1.5697	8.4 1.5697
8.4 1.5589	8.4 1.5589
8.4 1.5567	8.4 1.5567
8.4 1.5590	8.4 1.559
8.4 1.5550	8.4 1.555
9.4 1.5492	9.4 1.5492
9.4 1.5386	9.4 1.5386
9.4 1.5336	9.4 1.5336
9.4 1.5318	9.4 1.5318
9.4 1.5348	9.4 1.5348

10.5 1.5191	10.5 1.5191
10.5 1.5174	10.5 1.5174
10.5 1.51623	10.5 1.51623
10.5 1.51554	10.5 1.51554
10.5 1.51753	10.5 1.51753

PRESSURE 1

1.2 1.5160	1.2 1.516
1.2 1.5167	1.2 1.5167
1.2 1.51551	1.2 1.51551
1.2 1.51566	1.2 1.51566
1.2 1.51559	1.2 1.51559
2.15 1.51056	2.15 1.51056
2.15 1.5057	2.15 1.5057
2.15 1.50547	2.15 1.50547
2.15 1.50365	2.15 1.50365
2.15 1.5024100	2.15 1.50241
3.2 1.5061667	3.2 1.506166
3.2 1.5055852	3.2 1.505585
3.2 1.5031767	3.2 1.503176
3.2 1.5009753	3.2 1.500975
3.2 1.5016997	3.2 1.501699
4.2 1.5016970	4.2 1.501697
4.2 1.5013605	4.2 1.501360
4.2 1.4991280	4.2 1.499128
4.2 1.4996241	4.2 1.499624
4.2 1.4994408	4.2 1.499440
5.4 1.5026508	5.4 1.502650
5.4 1.5029381	5.4 1.502938
5.4 1.5050813	5.4 1.505081
5.4 1.4984923	5.4 1.498492
5.4 1.4946479	5.4 1.494647
6.4 1.4881287	6.4 1.488128
6.4 1.4831809	6.4 1.483180
6.4 1.4835359	6.4 1.483535
6.4 1.4821008	6.4 1.482100
6.4 1.4869445	6.4 1.486944
7.4 1.47885	7.4 1.47885
7.4 1.4709936	7.4 1.470993
7.4 1.4675858	7.4 1.467585
7.4 1.4699331	7.4 1.469933
7.4 1.4693774	7.4 1.469377
8.4 1.4648155	8.4 1.464815
8.4 1.4691300	8.4 1.46913
8.4 1.4696418	8.4 1.469641
8.4 1.46725326	8.4 1.467253
8.4 1.46758534	8.4 1.467585
9.4 1.4801128	9.4 1.480112
9.4 1.4823782	9.4 1.482378
9.4 1.4830091	9.4 1.483009

9.4 1.4854921	9.4 1.485492
9.4 1.4754417	9.4 1.475441
10.0 1.4870	10 1.487
10.0 1.4861	10 1.4861
10.0 1.4849461	10 1.484946
10.0 1.4819655	10 1.481965
10.0 1.4822735	10 1.482273
2.4 1.7236	2.4 1.7236
2.4 1.7258	2.4 1.7258
3.4 1.7237	3.4 1.7237
3.4 1.7218	3.4 1.7218
3.4 1.7221	3.4 1.7221
3.4 1.7213	3.4 1.7213
3.4 1.699188	3.4 1.699188
3.4 1.70	3.4 1.7
3.4 1.693	3.4 1.693
3.4 1.6190	3.4 1.619
3.4 1.5643186	3.4 1.564318
3.4 1.565885	3.4 1.565885
3.4 1.56408	3.4 1.56408
3.4 1.566	3.4 1.566
3.4 1.568	3.4 1.568
3.4 1.566	3.4 1.566
4.4 1.5473	4.4 1.5473
4.4 1.5496	4.4 1.5496
4.4 1.5484	4.4 1.5484
4.4 1.5528	4.4 1.5528
4.4 1.5524	4.4 1.5524
5.4 1.5455	5.4 1.5455
5.4 1.5479	5.4 1.5479
5.4 1.5467	5.4 1.5467
5.4 1.5481	5.4 1.5481
5.4 1.5463	5.4 1.5463
5.4 1.5458	5.4 1.5458
6.4 1.5446	6.4 1.5446
6.4 1.5472	6.4 1.5472
6.4 1.5447	6.4 1.5447
6.4 1.5508	6.4 1.5508
6.4 1.5447	6.4 1.5447
6.4 1.5433	6.4 1.5433
7.4 1.5420	7.4 1.542
7.4 1.5409	7.4 1.5409
7.4 1.5422	7.4 1.5422
7.4 1.5448	7.4 1.5448
7.4 1.5486	7.4 1.5486
8.4 1.5697	8.4 1.5697
8.4 1.5589	8.4 1.5589
8.4 1.5567	8.4 1.5567
8.4 1.5590	8.4 1.559
8.4 1.5550	8.4 1.555
9.4 1.5492	9.4 1.5492
9.4 1.5386	9.4 1.5386
9.4 1.5336	9.4 1.5336
9.4 1.5318	9.4 1.5318

9.4 1.5348	9.4 1.5348
10.5 1.5191	10.5 1.5191
10.5 1.5174	10.5 1.5174
10.5 1.51623	10.5 1.51623
10.5 1.51554	10.5 1.51554
10.5 1.51753	10.5 1.51753

PRESSURE -5

1.2 1.4808077	1.2 1.480807
1.2 1.4811967	1.2 1.481196
1.2 1.4806366	1.2 1.480636
1.2 1.4713888	1.2 1.471388
1.2 1.4709679	1.2 1.470967
2.2 1.4679536	2.2 1.467953
2.2 1.4634500	2.2 1.46345
2.2 1.4621151	2.2 1.462115
2.2 1.4640963	2.2 1.464096
2.2 1.45653012	2.2 1.456530
2.2 1.4696688	2.2 1.469668
3.2 1.4629143	3.2 1.462914
3.2 1.4689039	3.2 1.468903
3.2 1.4764370	3.2 1.476437
3.2 1.4697980	3.2 1.469798
3.2 1.4666350	3.2 1.466635
4.2 1.4553670	4.2 1.455367
4.2 1.4537872	4.2 1.453787
4.2 1.4532649	4.2 1.453264
4.2 1.49810	4.2 1.4981
4.2 1.4858780	4.2 1.485878
5.2 1.50567176	5.2 1.505671
5.2 1.5026300	5.2 1.50263
5.2 1.5035153	5.2 1.503515
5.2 1.4853928	5.2 1.485392
5.2 1.4715881	5.2 1.471588
6.2 1.4549817	6.2 1.454981
6.2 1.4548104	6.2 1.454810
6.2 1.4570586	6.2 1.457058
6.2 1.4528040	6.2 1.452804
6.2 1.4562089	6.2 1.456208
7.2 1.45867	7.2 1.45867
7.2 1.4578895	7.2 1.457889
7.2 1.4625519	7.2 1.462551
7.2 1.4656721	7.2 1.465672
7.2 1.4611255	7.2 1.461125
8.2 1.4722714	8.2 1.472271
8.2 1.4735937	8.2 1.473593
8.2 1.524790	8.2 1.52479
8.2 1.5099036	8.2 1.509903
8.2 1.5180321	8.2 1.518032
9.2 1.5119602	9.2 1.511960
9.2 1.5225266	9.2 1.522526

9.2 1.5210403	9.2 1.521040
9.2 1.4634617	9.2 1.463461
9.2 1.4659236	9.2 1.465923
10.2 1.4753459	10.2 1.475345
10.2 1.4835723	10.2 1.483572
10.2 1.4929003	10.2 1.492900
10.2 1.5061543	10.2 1.506154
10.2 1.5007532	10.2 1.500753
11.2 1.4865962	11.2 1.486596
11.2 1.4755400	11.2 1.47554
11.2 1.4919290	11.2 1.491929
11.2 1.4829704	11.2 1.482970
11.2 1.4953744	11.2 1.495374

PRESSURE -4

1.4 1.4946850	1.4 1.494685
1.4 1.4932859	1.4 1.493285
1.4 1.4930748	1.4 1.493074
1.4 1.4790496	1.4 1.479049
1.4 1.4756753	1.4 1.475675
2.4 1.4784779	2.4 1.478477
2.4 1.4876624	2.4 1.487662
2.4 1.4761319	2.4 1.476131
2.4 1.4719918	2.4 1.471991
2.4 1.48696	2.4 1.48696
3.4 1.4817901	3.4 1.481790
3.4 1.4802587	3.4 1.480258
3.4 1.4828329	3.4 1.482832
3.4 1.4832547	3.4 1.483254
3.4 1.4725543	3.4 1.472554
4.4 1.478944	4.4 1.478944
4.4 1.4796608	4.4 1.479660
4.4 1.4805700	4.4 1.48057
4.4 1.49011	4.4 1.49011
4.4 1.4863428	4.4 1.486342
8.4 1.4773317	8.4 1.477331
8.4 1.4854949	8.4 1.485494
8.4 1.4847164	8.4 1.484716
8.4 1.4831614	8.4 1.483161

PRESSURE VS DELTA F

10**-5

1.0 1.5170175	1 1.517017
1.0 1.5191	1 1.5191
1.0 1.5188	1 1.5188
1.0 1.5192	1 1.5192
1.0 1.5192	1 1.5192

1.0	1.5198
1.6	1.5195
1.6	1.5194
1.6	1.5193
1.6	1.5194
1.6	1.5195
1.6	1.5193
1.6	1.5191
1.6	1.5187
1.6	1.5185
1.6	1.5186
1.6	1.5186
1.6	1.5184
2.0	1.5180
2.0	1.5177
2.0	1.5174
2.0	1.5174
2.0	1.5173
2.0	1.5170
2.0	1.5168
2.0	1.5167
2.0	1.5159
2.0	1.5168
2.0	1.5159
2.0	1.5158
2.0	1.5158
2.0	1.4835
2.0	1.4834
2.0	1.4832
2.0	1.4834
2.0	1.4832
2.0	1.4831
2.0	1.4829
2.0	1.4827

1	1.5198
1.6	1.5195
1.6	1.5194
1.6	1.5193
1.6	1.5194
1.6	1.5195
1.6	1.5193
1.6	1.5191
1.6	1.5187
1.6	1.5185
1.6	1.5186
1.6	1.5186
1.6	1.5184
2	1.518
2	1.5177
2	1.5174
2	1.5174
2	1.5173
2	1.517
2	1.5168
2	1.5167
2	1.5159
2	1.5168
2	1.5159
2	1.5158
2	1.5158
2	1.4835
2	1.4834
2	1.4832
2	1.4834
2	1.4832
2	1.4831
2	1.4829
2	1.4827

PRESSURE 1
DELTA F VS DELTA T
HERTZ (10**3), VOTTS

945.5905	.028
941.2854	.029
937.8632	.030
935.3354	.031
931.8401	.032
927.9332	.034
924.0915	.034
919.7580	.036
914.4656	.036
909.3825	.036
904.6061	.036
900.2784	.037

945.5905	0.028
941.2854	0.029
937.8632	0.03
935.3354	0.031
931.8401	0.032
927.9332	0.034
924.0915	0.034
919.758	0.036
914.4656	0.036
909.3825	0.036
904.6061	0.036
900.2784	0.037

```
895.4626 .038                                    895.4626    0.038
888.8967 .040                                    888.8967     0.04
884.5370 .039                                     884.537    0.039
880.5563 .040                                    880.5563     0.04
846.2969 .052                                    846.2969    0.052
814.0041 .058                                    814.0041    0.058
795.9525 .063                                    795.9525    0.063
762.5305 .070                                    762.5305     0.07


PRESSURE 1
DELTA F VS DELTA T
HERTZ (10**3) DELTA F VS DELTA T
11/2/90 H. COCHRAN
733.5415 0.111                                   733.5415    0.111
729.0719 0.112                                   729.0719    0.112
723.8102 0.111                                   723.8102    0.111
701.8996 0.112                                   701.8996    0.112
688.6227 0.111                                   688.6227    0.111
687.6270 0.110                                    687.627     0.11
680.3535 0.108                                   680.3535    0.108
665.9808 0.105                                   665.9808    0.105
678.6007 0.112                                   678.6007    0.112
941.3456 0.116                                   941.3456    0.116
1.0139648 0.102    10**6 FOR DELTA F             1013964.    0.102
1.0279273 0.096                                  1027927.    0.096
1.0251640 0.080                                   1025164     0.08
902.2807 0.064    10**3 FOR DELTA F              902280.7    0.064
981.4863 0.102                                   981486.3    0.102
1.0327289 0.087   10**6 FOR DELTA F              1032728.    0.087
764.5773 0.052    10**3                          764577.3    0.052
672.6031 0.076                                   672603.1    0.076
658.9987 0.084                                   658998.7    0.084
650.3249 0.092                                   650324.9    0.092


DELTA F VS DEGREES C
DELTA F 10**3
11-6-90
858.5585 35.195                                  858.5585   35.195
865.9132 35.17                                   865.9132    35.17
888.8199 35.15                                   888.8199    35.15
899.3786 35.135                                  899.3786   35.135
910.0505 35.1                                    910.0505     35.1
933.0988 35.08                                   933.0988    35.08
941.8295 35.06                                   941.8295    35.06
964.8160 35.035                                   964.816   35.035
971.6840 35.025                                   971.684   35.025
976.7796 35.02                                   976.7796    35.02
1.0023567 35.10  10**6                           1002356.     35.1
1.0199866 35.005                                 1019986.   35.005
1.0086302 35.02                                  1008630.    35.02
```

Delta Frequency	Pressure
518.6	8.4 X 10E-9
517.7337	
517.7137	
517.7029	
517.7189	
517.8515	
517.7601	
517.8222	
517.7558	
517.7215	
517.7150	
517.9170	
517.8165	
517.7800	
517.7434	
517.8268	
517.7468	
517.60146	
517.58488	
517.56484	
517.53046	
517.52787	
517.52992	
517.51597	
517.50826	
517.50736	
517.50289	
517.49627	
517.49291	
517.48842	
517.491134	
517.49146	
517.49328	
517.48803	
517.49715	
517.11625	
517.08900	
517.09045	
517.09017	
517.09048	
517.09001	
517.08989	
517.53046	
518.67885	6.8 E-5
518.67330	
518.66894	
518.66601	
518.66347	
520.1487	

519.8906
519.6936
519.6214
519.6006
519.5610
518.8866
518.8861
518.8863
518.8860
518.8858
518.8855
518.8854
518.8851
518.8841
518.8849
518.8845
518.8843
518.8844
518.8845
518.8843
518.8835
518.8838
518.8833
518.8835
518.8834
518.8836
518.8835
518.8833
518.8833
518.8832
518.8830
518.8830
518.8828

518.31041
518.11847
517.99484
517.90684
517.84238

517.54808
517.54916
517.54978
517.55093
517.55171
517.57508
517.57560
517.57612
517.59269
517.59364
517.69072
517.69050

517.69189

519.36198
519.18984
519.08528
519.01783
519.07209
519.93221
519.89737
519.87011

VITA

Vickie Parker Gilbert was born in Fort Payne, Alabama on August 26, 1956. She attended elementary school in Henagar, Alabama and was graduated from Sylvania High School in 1974. She entered Northeast State Junior College, Rainsville, Alabama, in 1972 and was graduated from Auburn University, Auburn Alabama, in 1979 with a dual Bachelor of Science degree in Zoology and Secondary Science Education.

After teaching biology in the public school system, she re-entered The College of Engineering to obtain a Bachelor of Science in Chemical Engineering in 1986 from The University of Tennessee. She re-entered The Graduate School of The University of Tennessee, Knoxville, in September, 1987. She received the Master of Engineering degree, with major in Chemical Engineering in May 1992.

The author is a member of Phi Kappa Phi, Gamma Sigma Delta, Tau Beta Pi and the American Institute of Chemical Engineers. Ms. Gilbert is currently pursuing a doctorate in chemical engineering at The University of Tennessee, Knoxville.